Faculdade de Engenharia da Universidade do Porto

U. PORTO
FEUP FACULDADE DE ENGENHARIA
UNIVERSIDADE DO PORTO

Biomechanical Study of the Shoulder Joint Complex and Associated Injuries

Catarina de Sousa e Silva

September 2020

Faculdade de Engenharia da Universidade do Porto

U.PORTO
FEUP FACULDADE DE ENGENHARIA
UNIVERSIDADE DO PORTO

Biomechanical Study of the Shoulder Joint Complex and Associated Injuries

Catarina de Sousa e Silva

Dissertation carried out within the scope of
Master in Biomedical Engineering

Supervisor: Marco Paulo Lages Parente

Co-supervisor: João Pedro Sousa Ferreira

September 2020

Abstract

The glenohumeral joint allows the arm to perform countless and varied movements. This diversity generates a vulnerability on the joint, which, in turn, tends to suffer dislocations, affecting 1-2% of the population. In addition, individuals who frequently perform activities such as swimming, baseball, tennis, among others, are more likely to have shoulder injuries due to the stress to which their joints and muscles are subjected.

It is also known that, given a first dislocation, it may lead to the appearance of lesions in the structures that make up the shoulder joint complex, and some patients suffer from recurrent dislocations. Besides, recurrence can also be caused by the inability to choose the most appropriate treatment for each situation, due to the inaccuracy in the information available. It is important to note that a proper treatment should allow the patient to regain glenohumeral joint stability without causing pain and reducing mobility.

The development of this work aims to contribute to a better understanding of the shoulder complex, and thus provide relevant clinical information, allowing clinicians to understand which treatments are most appropriate for each situation with greater ease and confidence, ensuring that the patient will not suffer from instability in the glenohumeral joint again. A finite element model was built for this study, which allowed a biomechanical analysis of the shoulder joint complex.

This work allowed to verify the importance of the stabilizing role of the ligaments with the humerus positioned in the upper ranges. In addition, it was possible to conclude that glenoid defects with sizes greater than 37.5% of the glenoid width combined with any defect in the humeral head should be repaired with a Latarjet procedure.

Resumo

A articulação glenohumeral permite ao braço realizar inúmeros e variados movimentos. Esta diversidade gera uma vulnerabilidade por parte da articulação que, por sua vez, tende a sofrer luxações, afetando 1-2% da população. Além disso, indivíduos que realizam com frequência atividades como natação, beisebol, tênis, entre outras, têm maior probabilidade de sofrer lesões no ombro devido ao stress a que submetem as suas articulações e músculos.

Sabe-se ainda que, dada uma primeira luxação, esta poderá levar ao aparecimento de lesões nas estruturas que compõem o complexo articular do ombro, sendo que alguns pacientes sofrem de recorrência de luxações. Além disso, a recorrência também pode ser causada pela incapacidade na escolha do tratamento mais adequado para cada situação, devido à imprecisão das informações disponíveis. É importante notar que um tratamento adequado deverá devolver ao paciente a estabilidade da articulação glenohumeral sem causar dor e sem reduzir a mobilidade.

O desenvolvimento deste trabalho tem como objetivo contribuir para a melhor compreensão do complexo do ombro, e desta forma fornecer informação clínica relevante, permitindo aos clinicos perceber quais os tratamentos mais adequados para cada situação com maior facilidade e com mais confiança, assegurando que o paciente não irá voltar a sofrer de instabilidade na articulação glenohumeral. Para a realização deste estudo foi construido um modelo de elementos finitos, que permitiu uma posterior análise biomecânica do complexo do ombro.

Este trabalho permitiu verificar a importância do papel estabilizador dos ligamentos para posições do úmero com ângulos mais elevados. Além disso, foi possível concluir que defeitos na glenoide com tamanhos a partir de 37.5% da largura da glenoide combinados com qualquer defeito na cabeça do úmero deverão ser reparados com um procedimento de Latarjet.

Agradecimentos

Gostaria de começar por agradecer ao meu orientador, Professor Doutor Marco Parente, pelo acompanhamento ao longo destes últimos meses. Estou-lhe muito grata por toda a partilha de conhecimento e, acima de tudo, pela paciência e disponibilidade com que o fez.

À Doutora Ana Inês, pela disponibilidade para esclarecer alguns conceitos e por me famializar com os principais desafios enfrentados no tratamento de lesões que levam à instabilidade do ombro.

Aos meus pais e à Ruby por todo o apoio que me deram e por me incentivarem sempre a ser melhor.

Por fim, mas não menos importantes, um especial agradecimento à Inês, Mariana e Patricia pela amizade. Obrigada por me ouvirem, por me aconselharem e por me motivarem.

Contents

List of Figures

List of tables

Abbreviations, acronyms and symbols

FEA	Finite Elements Analysis
FEM	Finite Elements Method
ECM	Extracellular Matrix
IGHL	Inferior Glenohumeral Ligament
MGHL	Medial Glenohumeral Ligament
SHGL	Superior Glenohumeral Ligament
CT	Computed Tomography
MRI	Magnetic Resonance Imaging
SEDF	Strain Energy Density Function
HGO	Holzapfel-Gasser-Ogden
UMAT	User-defined material
DTD	Distance to dislocation
$\boldsymbol{u}$	Displacement
σ	Stress
ε	Strain

Chapter 1

Introduction

1.1 – Motivation

Biomechanics comes from "bios" and "mechanics". Mechanics is the study of physics of motion and how forces create that motion [1]. Therefore, biomechanics studies the structure and function of biological systems (which includes how bones, tendons, ligaments and muscles work together) through means derived from mechanics methodologies, being its main objectives to improve performance, to prevent injury and enable rehabilitation [2].

The shoulder has one of the most complex joints of the Human body (glenohumeral joint), enabling a wide range of different movements (including flexion, extension, abduction, adduction, external rotation and internal rotation). This joint presents a compromise between stability and mobility, which requires the interplay between the structures that compose it. Thus, in case any of the structures gets injured, it can lead to weakness, pain or instability [3].

There are many types of injuries that can occur on the shoulder, and these can be at the level of bones or soft tissues. The first includes fractures (broken bones), that usually occur due to an impact injury or dislocations (which occur when bones on opposite sides of a joint do not align), such as Hill-Sachs or/and Bankart lesions. On the other side, soft tissue injuries include bursitis, impingement syndrome, rotator cuff tear, frozen shoulder (also known as adhesive capsulitis), osteoarthritis [4].

It has been found that shoulder pain affects 18-26% of adults at any point in time [5] and that 1-2% of general population will experience a glenohumeral dislocation [6]. Regarding athletes, dislocations were reported to have and incidence of approximately 4-5% [7]. This is due to the fact that in overhead sports the repetitive stress can gradually lead to changes, such as stretching of the capsule, that in turn leads to hyperlaxity of the capsule which can cause instability or impingement [8]. Besides, it was reported that glenohumeral dislocations in the anterior direction correspond to 98% of all shoulder dislocations [9].

The incidence of recurrence after a first dislocation range from 14-100%, where patients under 20 years old have a recurrence rate of 72-100%, patients aged between 20-30 years have a recurrence of 70-82% and patients over 50 years have 14-22% of recurrence rate [10].

The main causes that lead to shoulder dislocation are sports practicing and traumas. Besides, some individuals are more likely to have dislocations due to factors such as age, gender and genetics (which may lead to weaker tendons) [11,12].

It is important to note that Bankart and Hill-Sachs lesions, which result from an anterior dislocation, are quite individualized, which means that these can have different sizes and locations. Besides, there is also a wide variety of treatments and little certainty as to which will be the most suitable for each case. Consequently, the treatment including immobilization and physical therapy has a recurrence rate that can exceed 70%, and the recurrence rate following surgical repair has been reported to be up to 17.5%. For cases that are subjected to surgical repair, patients may experience joint stiffness and reduced range of motion [13].

Furthermore, under-diagnosis and under-treatment are related to increased costs for society since these can lead to disability and loss of production and over-treatment can inflate health-care costs and even worsen the patient's condition [14].

Therefore, it is important for clinicians to understand the major anatomical structures and biomechanical functions associated with the shoulder complex to ensure that the evaluation sequence which is going to be planned is reliable, as well as the treatment steps [15].

The aim of these work is to better understand the mechanisms of the shoulder complex and the aetiology of shoulder instability, attempting to establish a validated algorithm that facilitates the choice of the most appropriate treatment for each case, providing stability without limiting the range of motion and, consequently, decreasing the recurrence rates. More specifically, we will focus on evaluating the stability of the glenohumeral joint with the presence of the Bankart and Hill-Sachs defects simultaneously, since it was reported that the recurrence is usually associated with the presence of both lesions [16].

The insights obtained through experimental biomechanics from cadaveric samples are relatively limited and it is impossible to test the combination of different defects at the glenoid and humeral head in a single cadaveric specimen, so a finite element approach was chosen. It is also important to note that this approach as some advantages since it is less expensive and more ethical [17].

1.2 –State of the art

In order to better understand the functioning of the shoulder complex, as well as the injuries that occur in it, studies have been conducted through in-vivo clinical reports, ex-vivo cadaveric work and using computer-based simulations.

In addition, it is known that Finite Element Analysis (FEA) has gained some popularity within biomechanics, with the number of articles increasing [18].

However, there are still some challenges faced when representing the shoulder using the Finite Elements Method (FEM), namely [18]:
- representation of the material properties of the shoulder tissues;
- definition of boundary and loading conditions;
- representation of all the structures that compose the shoulder and their interactions;
- validation of FE simulation results through in vivo experiments.

Nevertheless, the FEM has been applied to investigate the changes in glenohumeral joint contact stresses, caused by changes in the shape of humeral head and glenoid [18].

It has also been applied to study the biomechanical consequence of supraspinatus deficiency, focusing on the glenohumeral joint stability, which, if reduced, can lead to a secondary osteo-arthritis.

A model was built to aid shoulder joint replacement implantation. The results from this study revealed that computer models can be a great ally during the pre-operative planning, however the developed model still needs some improvements [19].

Furthermore, some studies attempted to understand the effect of Hill-Sachs and Bankart lesions on anterior stability. However, there is some inaccuracy in the data and, consequently, there is still no validated algorithm that can assist physicians in choosing the most appropriate treatment for each patient.

Some of these studies are briefly described below and include in-vivo, cadaveric and computational studies:

- In-vivo study with patients with anterior instability who underwent arthroscopic Bankart repair to assess the effect of glenoid bone loss on shoulder stability [20];

- A cadaveric study to assess the effect of glenoid lesions on anterior stability. A Bankart repair was done before performing the translation test, and they later concluded about the sizes of glenoid defects that can compromise shoulder stability and movement [21];

- A cadaveric study of simulated Hill-Sachs lesions to assess the effect of the size of the defects on the glenohumeral stability [22];

- A cadaveric study in which Hill-Sachs defects were created, followed by an osteoarticular allograft transplantation. This study aimed to conclude about which sizes of the Hill-Sachs lesions can lead to instability and therefore should be addressed with a bony procedure [23];

- A cadaveric study to assess the effect of bipolar lesions on the shoulder stability; Does not take into account the presence of soft tissues [9];

- A finite element shoulder model was used to investigate the effect of the presence of Bankart lesions and Hill-Sachs lesions simultaneously on shoulder instability. One of the limitations of this study includes not considering the presence of soft tissue [24];

Based on the information above, this work differs from what has already been done since it aims to create a FEM model with bipolar lesions without neglecting the presence of the glenohumeral capsule, which has an important stabilizing role.

1.3 – Document Outline

This dissertation begins with an introductory chapter that contains the motivation and objectives of the work, as well as a contextualization of the subject of study.

Chapter two describes the anatomy of the shoulder complex and the mechanisms that occur between the structures that compose it. Besides, this chapter also describes shoulder dislocations, more specifically the anterior dislocations, and the lesions that these may lead to. Finally, the treatment techniques available are presented, highlighting the problem of inaccurate information regarding the best treatment for different situations.

Chapter three presents an introduction to some concepts of solid mechanics and a theoretical explanation of the method used to develop the model.

Chapter four describes the methodology: explains how the 3D model was obtained; the material properties used, including a theoretical explanation of the constitutive models; finally, it describes the shoulder positions that were considered and the conditions and steps defined to run the simulations.

Chapter five presents the results and respective analysis.

Chapter six includes the conclusion and give some suggestions for future work.

Chapter 2

Shoulder Complex

2.1 – Anatomical Terminology

The anatomical position (in which the body stands upright, with the toes pointing forward and the feet parallel and at shoulder width) is a convention adopted to describe the spatial positions that all anatomical structures occupy [1].
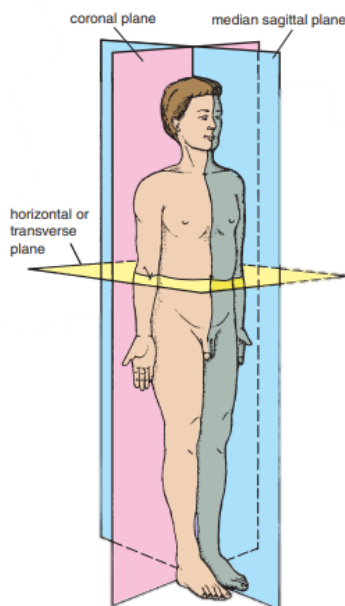
Figure 2.1 – Three planes of the body, adapted from [25].

As shown in figure 2.1, there are three planes most commonly used in anatomy, in order to make it easier to describe the motion of the structures that are part of the human body. These are described in Table 2.1.

Table 2.1 — The three planes of the body [26].

Plane	Description
Sagittal plane	Divides the body or an organ vertically into right and left sides.
Frontal (coronal) plane	Divides the body or an organ into an anterior portion and a posterior portion.
Transverse plane	Divides the body or organ horizontally into upper and lower portions.
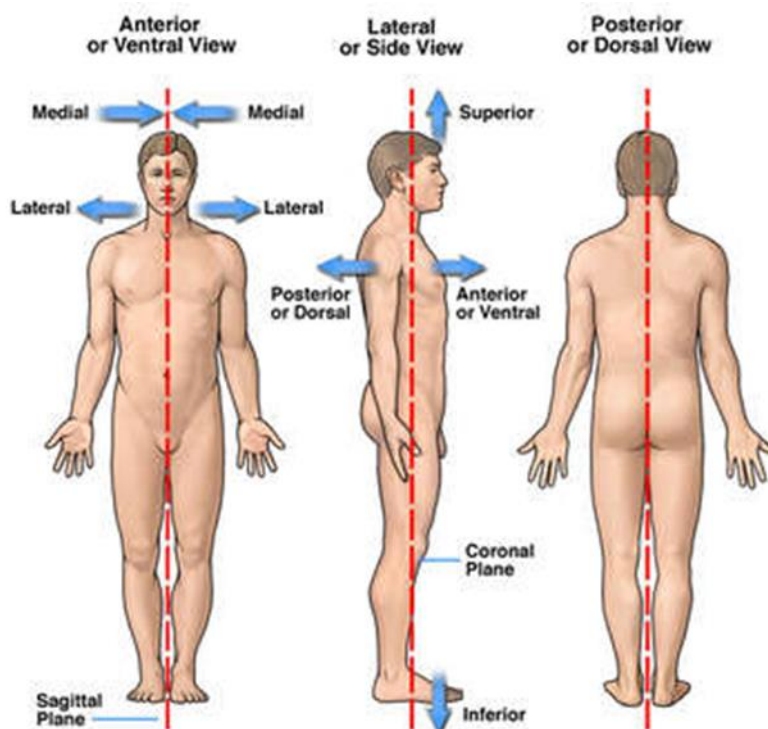
Figure 2.2 – Representation of the directional terms, adapted from [27].

The directional anatomical terms (shown in figure 2.2) are essential to describe the relative locations of different structures in the body and are described in Table 2.2.

Table 2.2 — The directional terms [25].

Directional Terms	Description
Anterior and posterior	Anterior refers to the front of the body and posterior refers to the back. For example, the toes are anterior to the foot.
Superior and inferior	Superior refers to a position above and inferior refers to a position below. For example, the pelvis is inferior to the abdomen.
Lateral and medial	Lateral describes the side of the body and medial describes the middle.
Proximal and distal	Proximal refers to a position in a limb that is nearer to the point of attachment and distal describes a position that is farther.
Superficial and deep	Superficial describes a position closer to the surface of the body and deep refers to a farther position.

2.2 – Shoulder anatomy

2.2.1 – Bones

The bones of the shoulder complex include the scapula, the humerus and the clavicle. The contact between the scapula and the humerus is promoted by the glenoid, as shown in figure 2.3.

(a) (b)
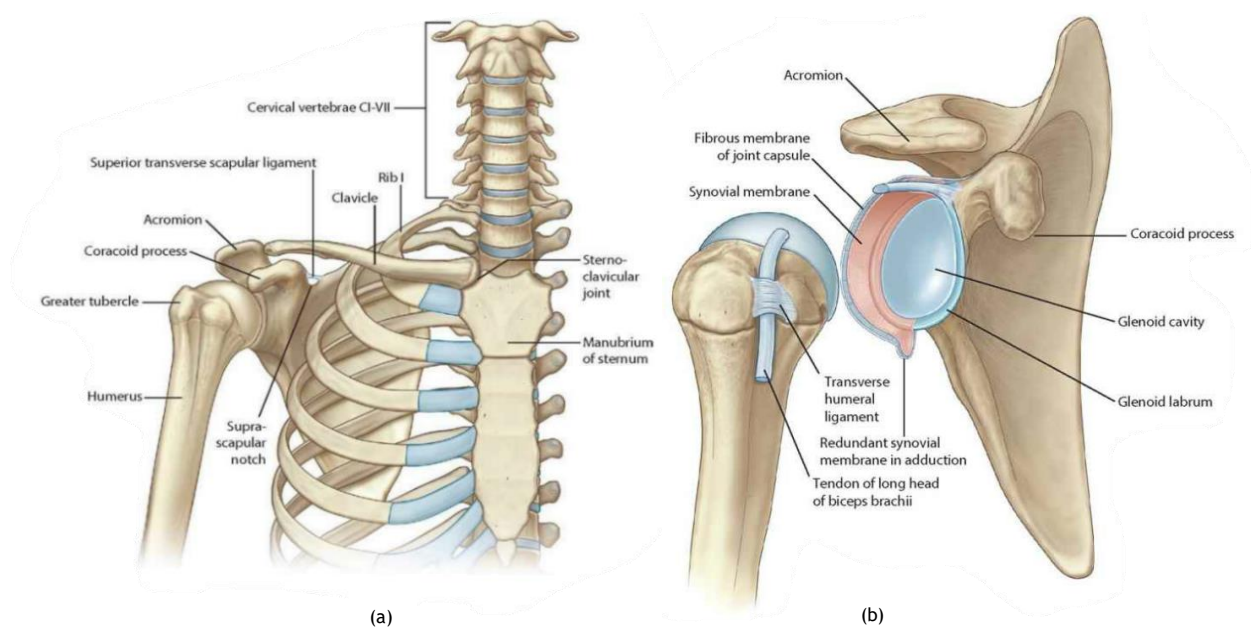
Figure 2.3 – Anterior view of the bony framework of the shoulder [28].

The humerus is the largest bone of the upper limb and it is divided into the head, anatomical neck, surgical neck and shaft, as shown in figure 2.4 (a). The humeral head has a 25°-35° retroversion in relation to the elbow condyles, it is described as a third of a sphere with a radius of approximately 25 mm, and it is the section of the humerus that articulates with the glenoid. The anatomical neck is where the capsule is attached, while the surgical neck marks the metaphysis of the bone. Besides, the greater and the lesser tubercles are sites for muscle attachment, and the intertubercular sulcus (which separates the 2 tubercles) is where the tendon of the biceps brachii is inserted [26, 29].

The scapula is one of the most important bones since it plays a crucial role in normal shoulder function. It has three important landmarks, which are the acromion, the coracoid process and the spine of the scapula, as shown in figure 2.4 (b). It is suspended on the axial skeleton by sternoclavicular ligaments, axioscapular muscles (which include the trapezius, rhomboids, serratus anterior and levator scapulae), coracoclavicular ligaments, atmospheric pressure and fascia [30] and it is positioned obliquely between the frontal and sagittal planes. It is a site for muscle attachment, a link in proximal to distal sequencing of the kinetic chain and it elevates the acromion to reduce impingement and coracoacromial arch compression while executing actions such as throwing [31].
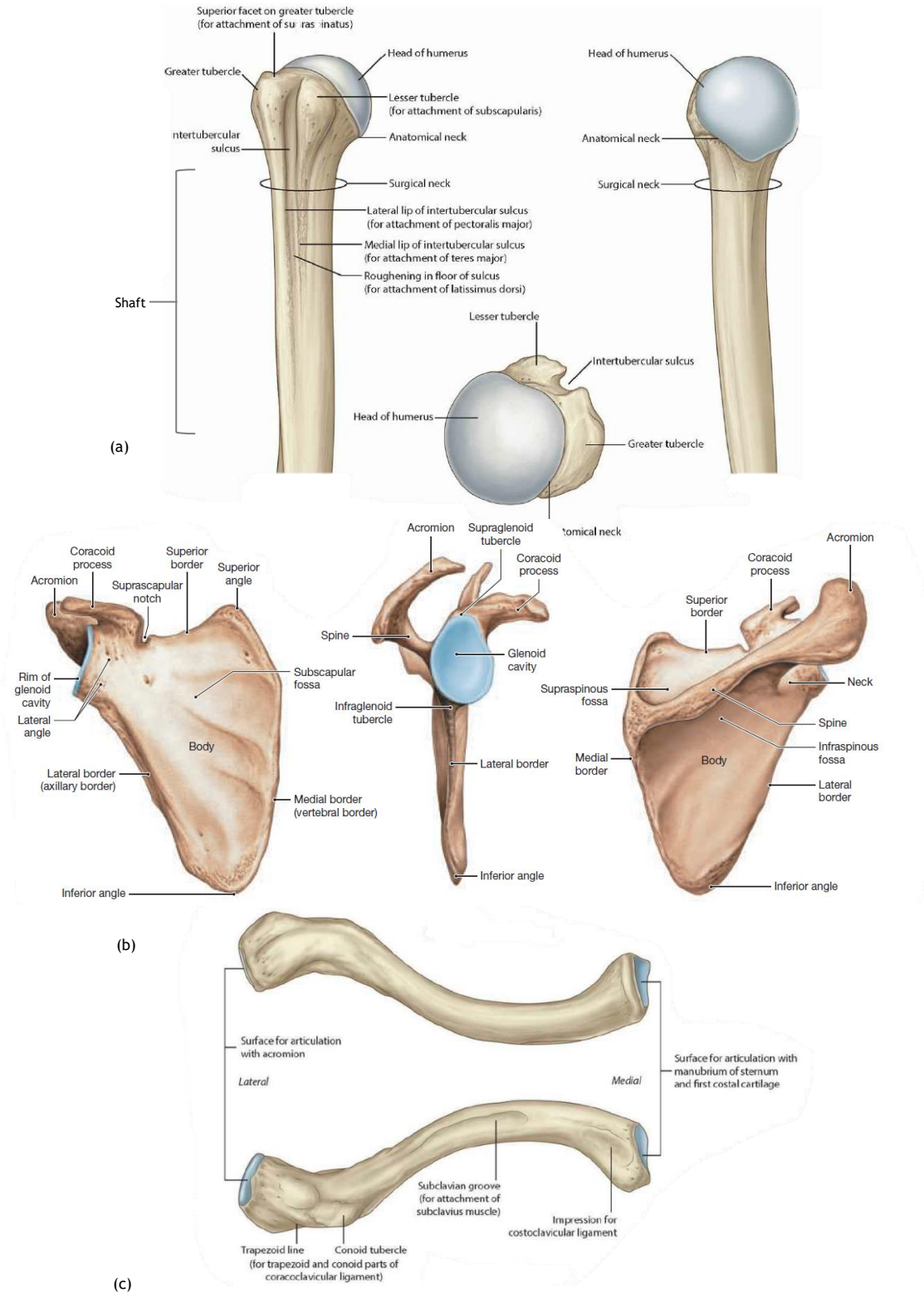
Figure 2.4 –Bony framework of the shoulder (a) humerus; (b) Scapula and (c) clavicle. Adapted from [26, 28].

The clavicle is a long curved bone, as shown in figure 2.4 (c), which articulates medially with the sternal manubrium and laterally with the scapula acromion [26].

2.2.2 – Joints

The shoulder complex is formed by four joints: acromioclavicular, sternoclavicular, scapulothoracic and glenohumeral.

The acromioclavicular joint is a plane synovial joint that joins the acromion of the scapula to the end of the clavicle, as shown in figure 2.5, and it contributes to the range of rotation of the scapula. It is formed by the articular disc and the acromioclavicular ligament [26].

The sternoclavicular joint is a plane synovial joint, and it articulates the clavicle to the manubrium of the sternum, as shown in figure 2.5. This joint is formed by the articular disc and the anterior and posterior sternoclavicular ligaments [26]. It contributes to the performance of several shoulder movements, such as shrugging, elevating the arm above the head and moving the shoulders back and forth [32].
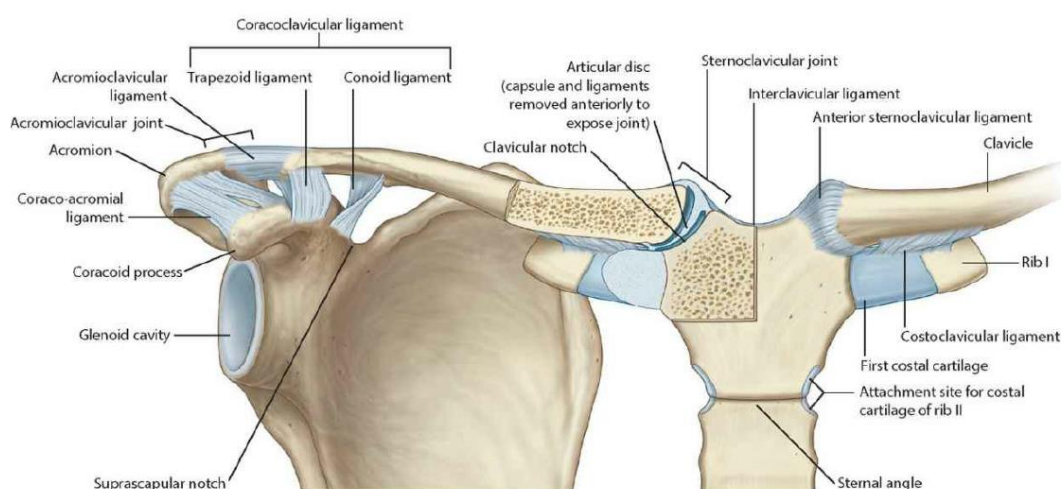
Figure 2.5 – Anterior view of the scapula and clavicle and respective ligaments and joints [28].

Before describing the glenohumeral and scapulothoracic joints, it is important to note that the combination of the movement of these two joints in a 2:1 ratio is essential to perform abduction of the arm. For instance, if the arm abducts 90°, the glenohumeral joint is responsible for rotating 60°, while the scapulothoracic joint rotates 30° [33].

The scapulothoracic joint connects the scapula to the thorax, as shown in figure 2.6, and consequently it allows the movement of the scapula against the rib cage [30].
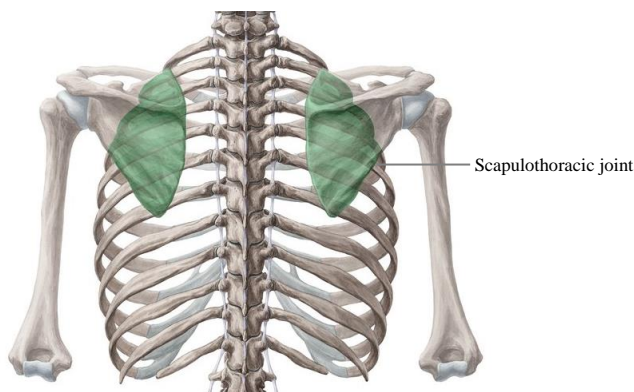
Figure 2.6 – Posterior view of the scapulothoracic joint. Adapted from[34].

The glenohumeral joint is a ball-and-socket synovial joint, that articulates the glenoid and the humeral head, as shown in figure 2.7. Since the humeral head has a larger surface than the glenoid, only 25% to 30% of the humeral head is in contact with it. Furthermore, the articular face of the humerus has a spherical shape, as mentioned above, while the glenoid fossa is pear-shaped (with a vertical diameter about 75% of the humeral head and a transverse diameter of 55% of the humeral head). These aspects cause the surfaces to be incongruent, and the joint loose-packed. In contrast, the articular cartilage of the glenoid (which consists of hyaline cartilage) is thickest in the periphery and thinnest in the center, opposite to the articular cartilage of the humeral head, favoring the fitting of the humerus into the glenoid [4].

This joint is characterized for being more suited for mobility than stability, which in turn leads to it being more commonly dislocated. For this reason, the presence of static and dynamic stabilizers is essential. The static stabilizers include the bones, the glenoid labrum, the glenohumeral ligaments along with the joint capsule and the negative intra-articular pressure, while the dynamic include the rotator cuff muscles and other surrounding muscles that compress the humeral head into the glenoid [35]. In addition, this joint also includes the coracohumeral ligament and the transverse humeral ligament.
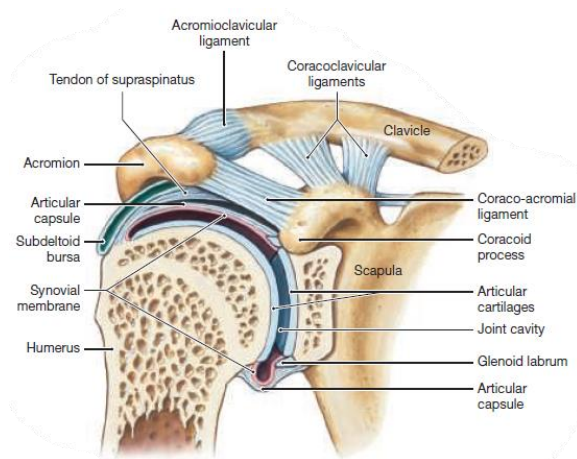
Figure 2.7 –Anterior view of the frontal section of the glenohumeral joint [26].

The capsule is relatively thin, mainly in the posterior section. It attaches to the anatomical neck of the humeral head, and to the outer surface of the labrum. It is covered with synovium inside and the glenohumeral ligaments outside reinforce the structure. An injury on the capsule may have an adverse effect on joint function, in other words, a contracture of the postero-superior section may limit internal rotation and flexion, while a contracture of the antero-inferior may limit the external rotation of the abducted arm [36].

The labrum is a ring of triangular shape, which consists of fibrocartilage, and it is attached to the periphery of the glenoid. The inferior section is firmly attached to the glenoid while the superior portion is more loosely attached, allowing a range of motion of the humerus in relation to the glenoid. It helps increasing the contact surface between the humeral head and the glenoid and its shape adapts in order to enable the rotation of the humeral head. It enhances shoulder stability by limiting the translation of the humeral head, increasing the depth of the glenoid cavity by 50% and consequently increasing the concavity-compression effect. Besides, it also acts as a binding site for the glenohumeral ligaments. Finally, it is important to note that 10 to 20% of the stabilization forces on the glenohumeral joint are caused by the labrum [37].

The negative intra-articular pressure, generated by the sealed capsule with limited volume, creates a vacuum effect, which helps in preventing excessive translation [29].

The synovial fluid inside the capsule allows the interaction between the humeral head and the glenoid to occur smoothly and without pain, providing the cohesion and adhesion effect [29], where adhesion is described as the fluid retention on a surface and cohesion is the bonding of two surfaces by fluid [38].

2.2.3 – Ligaments

Ligaments are specialized connective tissues, responsible for connecting the bones of the human body. They consist of 80% extracellular matrix (ECM) and 20% fibroblast cells [39], and their hierarchical structure is represented in figure 2.8. Fibroblast cells are responsible for secreting collagen fibers and ground substance that constitutes the ECM.

The ground substance is composed of polysaccharides and proteins like elastin and its functions include water storage, serve as a medium for intercellular exchange and support the cells.

Collagen fibers are defined as closely packed bundles of fibers parallel oriented, providing mechanical resistance. Their properties vary with some factors such as temperature, aging and exercise.
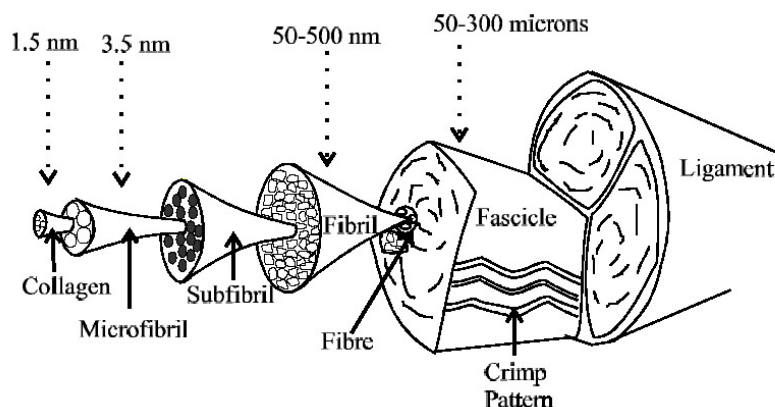
Figure 2.8 – Hierarchical structure of ligaments [40].

Figure 2.9 shows the typical stress-strain curve of ligaments, which are highly anisotropic, presenting the following characteristics: stiffness to compression, bending and low resistance.

Besides, ligaments have history- and time-dependent viscoelastic properties, which means that they are affected by the frequent performance of intense activities and by the different load conditions to which they are subjected during the performance of the activities [41].

The ligaments have a range of strains having minimal resistance to movement, that allows the individual to perform different movements. However, when the strain in the ligaments increases and that range is exceeded, the collagen fibers change their "crimped" state to a straightened state [41]. Therefore, when the shoulder is subjected to excessive external rotation, the antero-inferior glenohumeral ligament has a 30% increase in its length [42].
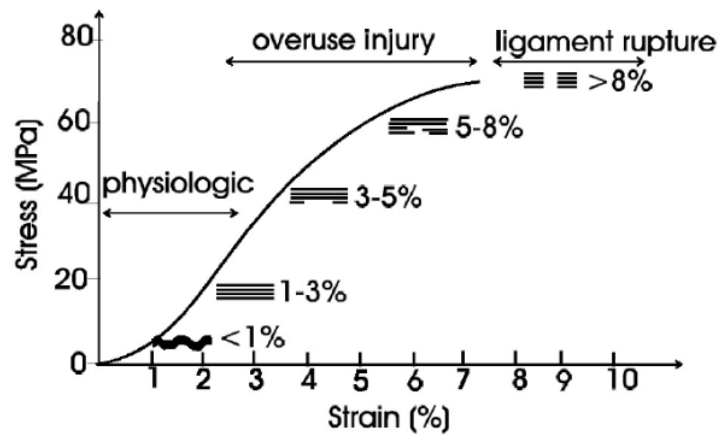
Figure 2.9 – Typical Stress-Strain curve of ligaments [40].

The glenohumeral ligaments, shown in figure 2.10, are important to provide a barrier against translation of the humeral head and to increase compressive forces of the joint. However, not to over-restrain the joint, these are lax in most of the functional range of the shoulder [43].
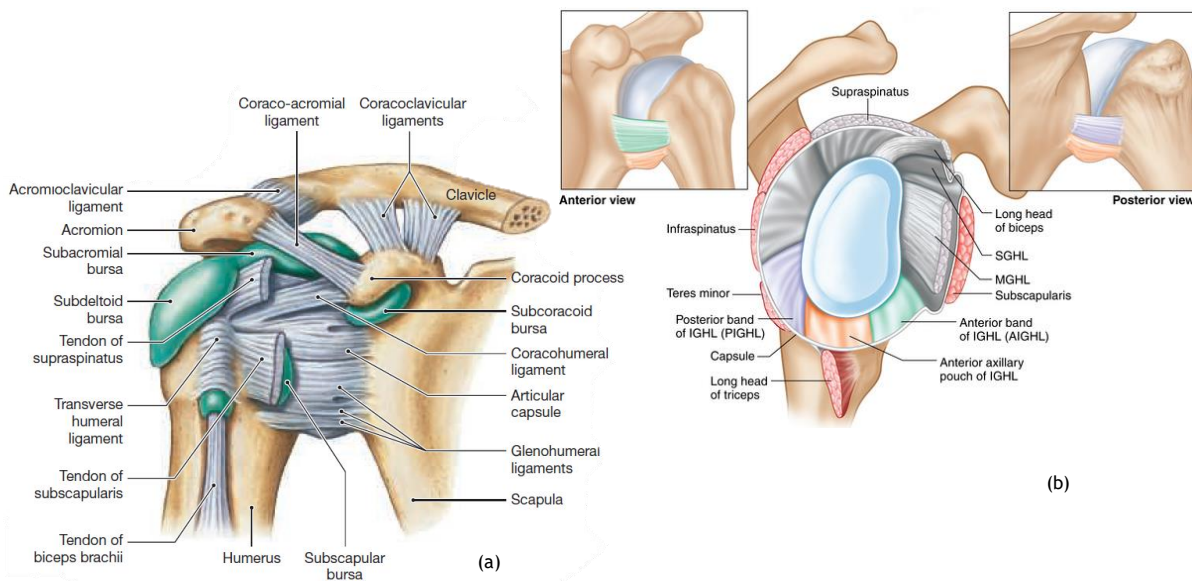
Figure 2.10 – (a) Anterior view of the right shoulder joint (b) Lateral view of the glenohumeral ligaments [26, 44]

The glenohumeral ligaments are subdivided into the inferior glenohumeral ligament (IGHL), the middle glenohumeral ligament (MGHL) and the superior glenohumeral ligament (SGHL) [35, 45].

The IGHL is the thickest and can be divided into the anterior band (which strengthens the capsule in the anterior portion), axillary pouch (which is thinner and broader), and the posterior band. It is attached to the anatomical neck of the humerus in a V- or U- shape. This ligament restrains anterior and inferior dislocation, particularly during abduction, extension and external rotation.

The MGHL can be thin or thick, originates from the anterior labrum and inserts into the lesser tuberosity. It is an anterior stabilizer of the glenohumeral joint, acting during adduction and during abduction at 30°-45°.

The SGHL is variable in origin and size. It resists inferior translation when the arm is in the adduction position and without rotation. Besides, it limits the external rotation of the arm in adduction together with the coracohumeral ligament.

The coracohumeral ligament also resists posterior and inferior translation when the shoulder is suspended. In addition, it stabilizes the shoulder complex when performing the abduction movement [35].

The transverse humeral ligament is responsible for keeping the tendon of the long head of the biceps in the bicipital groove [26].

Table 2.3 shows the primary and secondary restrictions regarding anterior stability with the arm in different positions.

Table 2.3 —Ligaments that contribute to the anterior stability of the glenohumeral joint, with the arm in different positions [4].

Arm position	Primary constraints	Secondary constraints
0°	MGHL and SGHL	Posterior capsule
45° of abduction	MGHL	Posterior capsule and IGHL
90° of abduction	IGHL	Posterior capsule and MGHL
External rotation at 90° of abduction	IGHL	-
Internal rotation at 90° of abduction	IGHL	-

2.2.4 – Muscles

As mentioned above, muscles are important since they play the role of dynamic stabilizers of the glenohumeral joint (passive force). But they are also responsible for generating the force required to perform daily movements (active force).

The scapulothoracic muscles (latissimus dorsi, serratus anterior, pectoralis major and deltoid) present a greater distance from the glenohumeral joint, however they are also responsible for its stability, as they can generate large moments around the shoulder joint due to their anatomy and the distance they have from the center of rotation [35].

In contrast, the rotator cuff muscles (supraspinatus, infraspinatus, teres minor and subscapularis) are located near the center of rotation and act in conjunction with the glenohumeral ligaments. These muscles withstand the shearing forces that occur in the glenohumeral joint, center the humeral head in the glenoid and maintain the compressive force, as shown in figure 2.11. Therefore, if rotator cuff muscle forces decrease by 50%, it leads to approximately 50% increase in anterior dislocation [38].
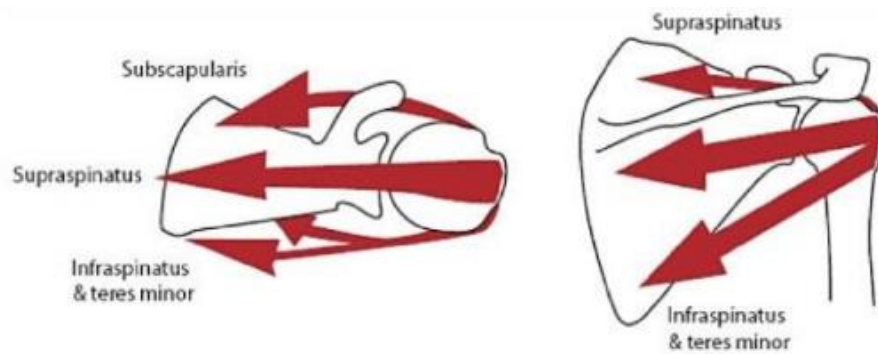
Figure 2.11 – Representation of the influence of the rotator cuff muscles on the shoulder complex [38].

The muscles that compose the shoulder complex are shown in the figure below, and the tables 2.4, 2.5 and 2.6 describe their origin, insertion and actions.
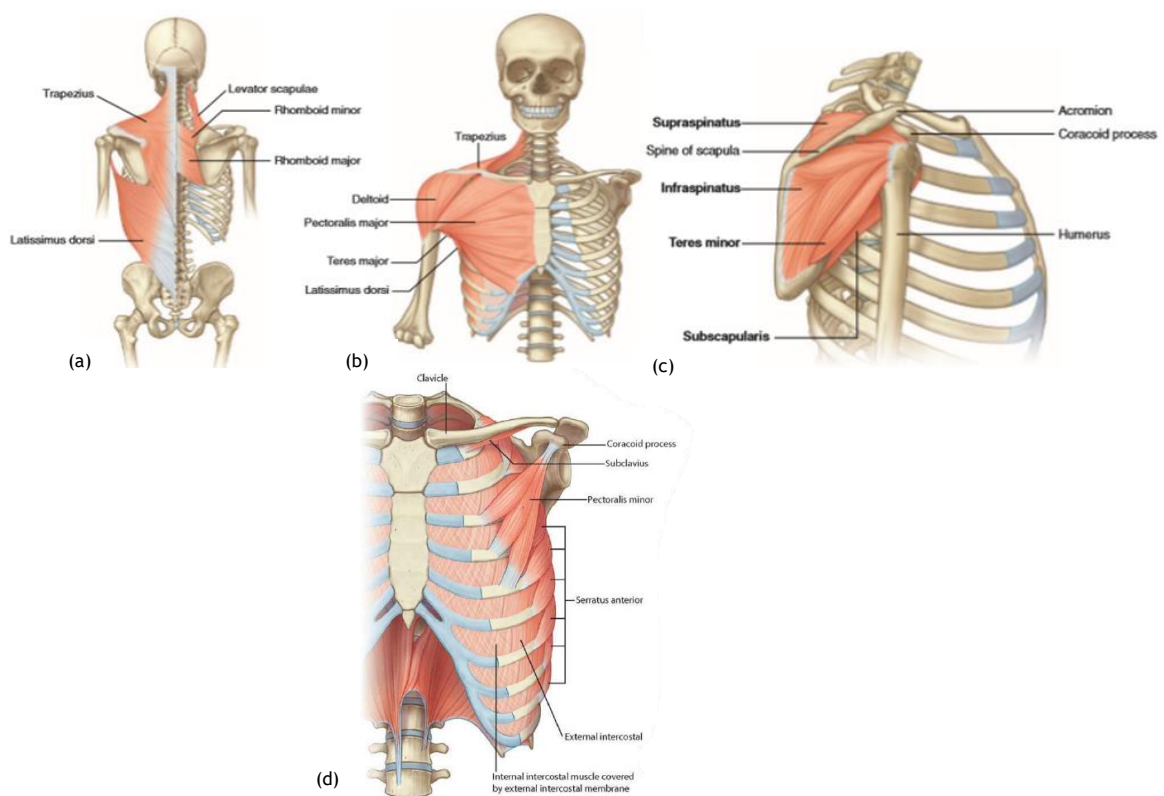
Figure 2.12 – Representation of the muscles on the shoulder complex (a) posterior view, (b) anterior view, (c) lateral view and (d) anterior view of the deep muscles [28, 30].

Table 2.4 — Muscles connecting the upper limb to the rib cage [26].

Muscle	Origin and Insertion	Action
Pectoralis minor	**Origin:** Anterior surfaces and superior margins of ribs 3–5 or 2–4 and the fascia covering the associated external intercostal muscles **Insertion:** Coracoid process of scapula	Depresses and protracts the shoulder; Rotates the scapula so glenoid cavity moves inferiorly (downward rotation).
Pectoralis major	**Origin:** Cartilages of ribs 2–6, body of sternum, and inferior, medial portion of clavicle **Insertion:** Crest of greater tubercle and lateral lip of intertubercular sulcus of humerus	Flexes, adducts and medially rotates the upper limb.
Subclavius	**Origin:** First rib **Insertion:** Clavicle (inferior border of middle 1/3)	Anchors and depresses the clavicle.
Serratus anterior	**Origin:** Anterior and superior margins of ribs 1–8, 1–9, or 1–10 **Insertion:** Anterior surface of vertebral border of scapula	Rotates the scapula, allowing the arm to be raised over 90°; Holds the scapula against the rib cage.

Table 2.5 — Muscles connecting the upper limb to the spine [26].

Muscle	Origin and Insertion	Action
Trapezius	**Origin:** Occipital bone, ligamentum nuchae, and spinous processes of thoracic vertebrae **Insertion:** Clavicle and scapula (acromion and scapular spine)	Elevates the scapula; Rotates the scapula during abduction of the arm; Retracts the scapula; Pull the scapula inferiorly.
Levator scapulae	**Origin:** Transverse processes of first four cervical vertebrae **Insertion:** Vertebral border of scapula near superior angle and medial end of scapular spine	Elevates the scapula.
Rhomboid major	**Origin:** Ligamentum nuchae and the spinous processes of vertebrae T2 to T5 **Insertion:** Vertebral border of scapula from spine to inferior angle	Retracts and rotates the scapula.
Rhomboid minor	**Origin:** Spinous processes of vertebrae C7–T1 **Insertion:** Vertebral border of scapula	Retracts and rotates the scapula.
Latissimus dorsi	**Origin:** Spinous processes of inferior thoracic and all lumbar and sacral vertebrae, ribs 8–12, and thoracolumbar fascia **Insertion:** Floor of intertubercular sulcus of the humerus	Extends, adducts, and medial rotates the upper limb.

Table 2.6 — Muscles associated to the scapula [26,35].

Muscles	Origin and Insertion	Action
Deltoid	**Origin:** Clavicle and scapula (acromion and adjacent scapular spine) **Insertion:** Deltoid tuberosity of humerus	Abducts the humerus (major abductor of the arm); Flexes and medially rotates the humerus; Extends and laterally rotates the humerus.
Supraspinatus	**Origin:** Supraspinous fossa of scapula **Insertion:** Greater tubercle of humerus	Abducts the arm 0-15°; Assists deltoid for 15-90°.
Infraspinatus	**Origin:** Infraspinous fossa of scapula **Insertion:** Greater tubercle of humerus	Avoids excessive posterior and/or superior translation of the humerus; Generates about 60% of the external rotation force.
Subscapularis	**Origin:** Subscapular fossa of scapula **Insertion:** Lesser tubercle of humerus	Resists anterior and inferior translation. Acts as an internal rotator.
Teres major	**Origin:** Inferior angle of scapula **Insertion:** Medial lip of intertubercular sulcus of humerus	Adducts, extends and medially rotates the humerus.
Teres minor	**Origin:** Lateral border of scapula **Insertion:** Greater tubercle of humerus	Resists superior and posterior translation; Generates 45% of external rotation force.

Rotator cuff injuries are frequent and can occur in response to fatigue stress. In case of supraspinatus paralysis, the deltoid compensates by generating more force, as shown in figure 2.13 (c), whereas if the opposite happens then 50% of abduction strength is lost [45].
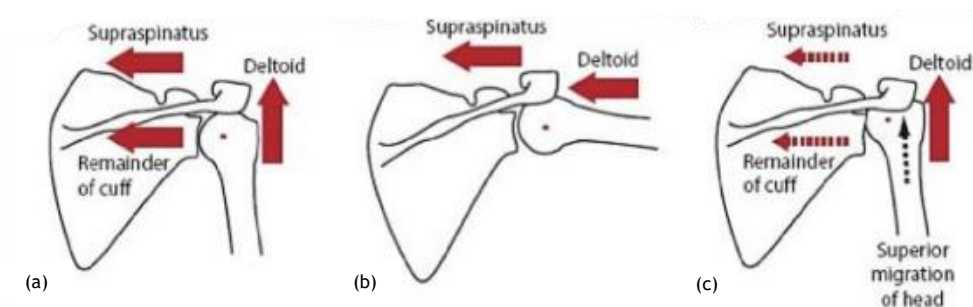
Figure 2.13 – Forces caused by the rotator cuff and deltoid muscles on the shoulder complex a) at initiation of abduction, b) at 90 degrees of abduction and c) in a presence of weak rotator cuff muscles [38].

2.3 – Shoulder biomechanics

Shoulder movement comprises six isolated movements: flexion, extension, abduction, adduction, external rotation and internal rotation. Flexion and extension occur in the sagittal plane and describe the forward and backward motion of the arm, respectively. Abduction and adduction take place in the frontal plane and describe the lateral motion of the arm, in which abduction refers to the upward motion and adduction to the downward motion. Internal and external rotation occur through the long axis of the arm (encompassing an infinite number of planes). Finally, there is also horizontal adduction and abduction which refers to the arm movement in the medial and lateral direction, respectively, and for a given degree [26].

It is important to note that the plane of the scapula translates forward during elevation, since it is not fixed, as shown in figure 2.14 [30].
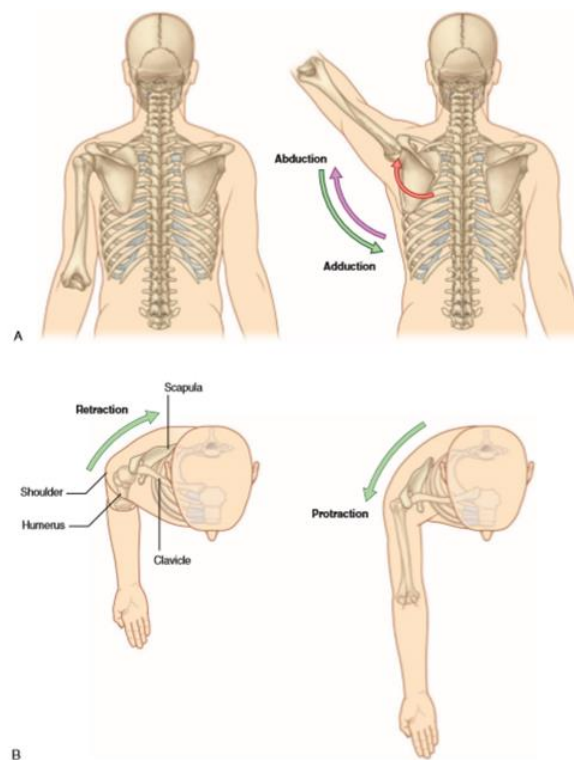
Figure 2.14 – Representation of the scapula orientation while performing different movements [30].

When the humerus is elevated up to 30° of abduction and 60° of flexion, the scapula moves to find a position of stability [4]. The initial phase is individualized and, after this phase, the scapula rotates and the center of rotation shifts toward the glenoid, which ends up oriented anteriorly towards the sagittal plane. Therefore, the scapular movement is very important as it allows the adjustment of the glenoid, acting as a stable platform for the humeral head. Through these movements the scapula rotates approximately 60°. Thus, stability of the glenohumeral joint is maximum as the glenoid accommodate the humeral head. If scapular rotation was not possible, the arm would not be able to actively raise beyond 90° of abduction [4].

Regarding stability, different situations involve different structures. In other words, the negative intra-articular pressure helps to stabilize the glenohumeral joint, when the arm is at rest and during motion in the mid- range. Besides, in mid- range the concavity-compression

effect promoted by muscle contraction also plays an important role. Finally, the glenohumeral ligaments are the most important stabilizers in the end range [37]. The following table has more detailed information on which structures stabilize the glenohumeral joint with the arm in different positions.

Table 2.7 — Stability of the glenohumeral joint. Adapted from [4].

Position	Structure
Lower range (0°-45°)	Anterior capsule
	SGHL
	MGHL
	Coracohumeral ligament
	Subscapularis, infraspinatus and teres minor muscles
Middle range (45°-75°)	MGHL
	Subscapularis, infraspinatus and teres minor muscles
	IGHL
Upper range (>75°)	IGHL

Massimini *et al*, 12 [43] studied the translations of the humeral head in-vivo and obtained the following results: for healthy and young individuals, the humeral head translates 4.8 ± 4.4 mm anteriorly and 1.6 ± 1.4 mm superiorly as the angle of abduction increases from 0° to 45° and translates 3.2 ± 2.8 mm anteriorly and 0.3 ± 2.1 mm superiorly at 90° of abduction. During maximum external rotation at 90° abduction, the humeral head translates 4.7 ± 3.2 mm anteriorly and 1.6 ± 3.3 mm superiorly, while for maximum internal rotation it translates 1.2 ± 4.6 mm posteriorly and 0.9 ± 2.6 mm inferiorly.

Due to the configuration of the glenoid, the anterior-posterior translation of the humeral head is bigger than the translation on the superior-inferior direction. Furthermore, the force necessary to produce a dislocation is approximately 60% of the compressive force in the superior-inferior direction and 35 % in the anterior – posterior direction.

Three types of forces act on the shoulder promoted by the muscles, which are compressive forces (that stabilize the glenohumeral joint), and shear forces, which includes forces in two different directions (and have the opposite effect on the glenohumeral joint). By measuring the ratio between the shear forces and the compressive forces, we can quantify the glenohumeral joint stability as shown in equation 2.1 [4].

$$stability\ ratio = \frac{shear\ force}{compressive\ force} \qquad (2.1)$$

Dislocations occur when the shear forces exceed the stabilizing capacity of the joint.

The understanding of the relationships between the structures that compose the shoulder is essential for the successful diagnosis and treatment of shoulder injuries.

2.4 – Shoulder dislocations

Shoulder dislocations can occur in the anterior direction (which corresponds to 98% of all shoulder dislocations [9]), as well as in the posterior and inferior directions, depending on the orientation of the external destabilizing force. These may lead to deformation of the gleno-humeral ligaments, antero-inferior labral lesions and bony injuries that consequently result in recurrent instability.

Shoulder subluxations are characterized by the humeral head partially sliding in and out of place.

According to the literature, anterior dislocations usually occur in the apprehension position (when the humerus is 60º abducted and 60º externally rotated) [46]. These can lead to failure of the IGHL. However, since IGHL can stretch considerably before ligament failure, some patients might have a subluxation without disruption of the capsule [4].

A Bankart lesion consists of the detachment of the antero-inferior section of the labrum, as shown in figure 2.15, and can also involve some bone loss (bony Bankart lesion) from the glenoid rim. A study reported that these lesions occur in up to 95% of the shoulders that had a dislocation [47]. Another study concluded that up to 86% of patients with recurrent instability have a glenoid defect [48]. These injuries cause a decrease in pressure caused by the anterior band of the IGHL, which reduces the ability of these ligaments to maintain the humeral head in the glenoid fossa, especially when performing more demanding movements such as external rotation [49]. However, it was reported that if the joint capsule is "strong and good quality" the episode of instability will not cause meaningful stretching to it, in contrast to a "weak" capsule which will consequently lead to recurrent subluxations and dislocations [50]. Besides, the defect in the antero-inferior portion of the glenoid rim reduces the concavity of the glenoid, which leads to reduction of the concavity-compression effect, reducing the ability of the shoulder to resist external forces that lead to dislocation [49].
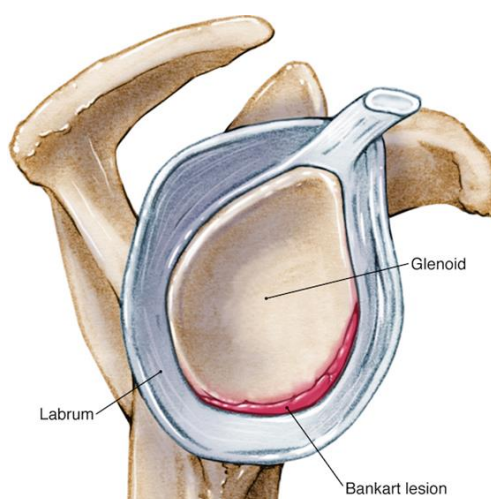
Figure 2.15 – Representation of the Bankart lesion [51].

Studies have shown that among the 3 sites of failure for the IGHL, 40 % occur in the glenoid insertion, 35% in the ligament's midsubstance and 25 % in the humeral insertion [52]. When it occurs at the level of the glenoid insertion, it represents a Bankart lesion.

Another common shoulder injury is the Hill-Sachs lesion which can be defined as a cortical depression in the postero-superior section of the humeral head, as shown in figure 2.16. These

were reported to occur in up to 90% of shoulders that had a dislocation [47]. And, for shoulders with recurrent instability these are present in up to 100% [49].

As with Bankart's lesion, when the shoulder has a Hill-Sachs lesion the probability of a new dislocation may increase because the ligaments and the labrum may have been injured during the first dislocation, failing to perform their function as stabilizers.

A concept that is used to assist in the identification of engaging Hill-Sachs lesions, which subject the shoulder to recurrent dislocation, is the glenoid track [53]. The glenoid track is the contact zone between the superolateral aspect of the humeral head and the glenoid during abduction, horizontal extension and external rotation [54]. Thus, this concept consists of verifying whether a Hill-Sachs lesion engages or not with the glenoid. A lesion is classified 'on-track' if it does not engage with the glenoid and, consequently, cannot cause dislocation. While a 'off-track' lesion has a risk of engaging and will lead to recurrent instability.

As the number of dislocations increases, the risk of injury/increasing the size of an existing injury also increases and, consequently, the risk of recurrence is higher. Nevertheless, it has been reported that after a first dislocation 56% of patients experience recurrent instability [55].
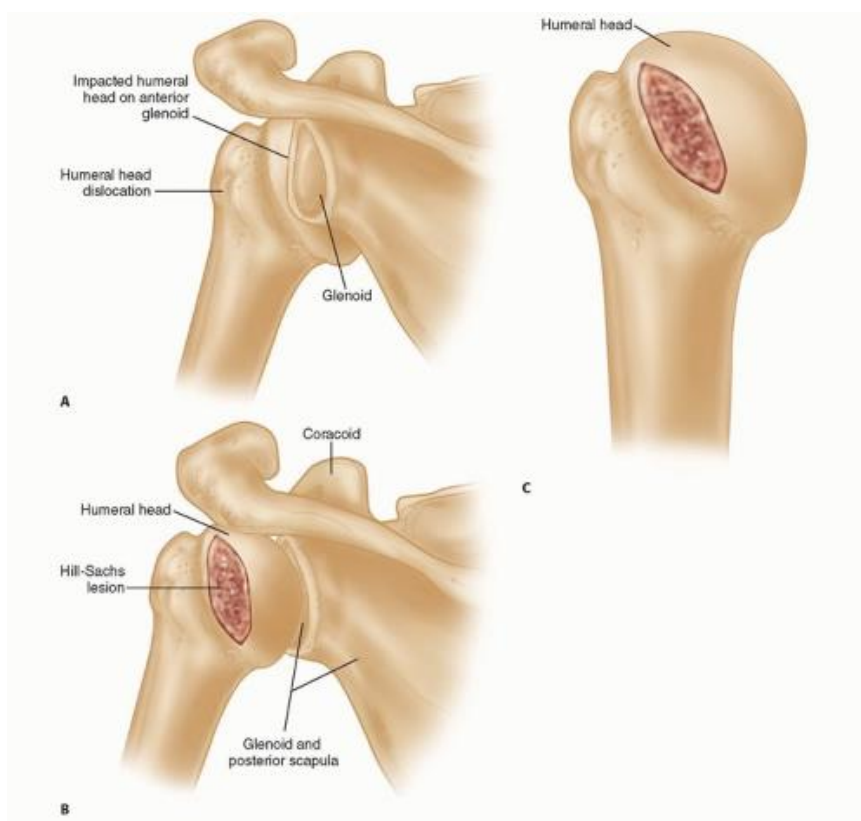
Figure 2.16 – Representation of the Hill – Sachs lesion [56].

Bankart and Hill-Sachs lesions are more likely to co-occur (than occurring in isolation) and it was documented that 61.8% of the patients with recurrent anterior instability had combined defects [16]. Besides, as Bankart lesions become larger, the size of the defects on the humeral head also increase (although the sizes of both lesions do not show a strong correlation). It is important to note that the bigger the lesions, smaller the contact area gets and so the instability increases.

Of patients undergoing surgical treatment for anterior instability, 65-97% were reported as having a Bankart lesion, 90% a Hill-Sachs lesion, 13% a rotator cuff tear and 10% a superior labral anterior posterior (SLAP) or posterior labral tears [4].

2.5 – Diagnostic and Treatments

2.5.1 - Diagnostic

The diagnosis can be made using the patient's history and medical exams, such as computed tomography (CT) and Magnetic Resonance Imaging (MRI). It has been shown that 3D CT was able to positively predict the need to undergo Latarjet repair for 96% of patients [57] and MRI has an accuracy of 100% for the diagnosis of osteochondral defects and 90% for the diagnosis of Bankart lesions [58]. Besides, there is the possibility of resorting to physical exams such as the Gagey's, apprehension and Jobe relocation tests. The apprehension and Jobe relocation tests were shown to have a positive predictive value of 96% to identify anterior shoulder instability [59].

The Gagey test is indicative of laxity of the inferior glenohumeral ligaments if there is asymmetric hyperabduction with a difference greater than 15° from the contralateral shoulder [59].

The apprehension test allows to assess the instability of the glenohumeral joint in the anterior direction. It begins with the patient in supine position, and the arm must be abducted 90°, with the elbow flexed 90° and the humerus must have neutral rotation. Then, the therapist causes external rotation of the humerus, holding the wrist of the patient. The test is considered positive if the patient shows apprehension in any way.

If the apprehension test is positive, the therapist may apply a force in the posterior direction. Thus, the Jobe relocation test is positive if the patient's pain or apprehension is reduced when applying this pressure. When this test is positive, the patient can be diagnosed with glenohumeral instability, dislocation or impingement [60].

Failures in diagnosis can lead to inadequate selection of the procedure, which, consequently, can lead to recurrence. In fact, it has been demonstrated that failure to identify and address both the Bankart and Hill-Sachs injuries can lead to shoulder instability rates as high as 67% [49].

2.5.1 - Treatments

Treatment may involve non-surgical rehabilitation or surgical repair. The first approach usually involves an immobilization period of approximately 3 weeks and it is followed by a rehabilitation period, in which the patient gradually returns to daily activities [14]. Surgical techniques are used when the injury is more severe, and these include anatomic or intracapsular repairs, which attempt to repair and reinsert the labrum and the ligaments in their original position (e.g. Bankart repair) and nonanatomic or extracapsular repairs, which consist of reconstructing the glenohumeral joint with a bone block (Bristow or Latarjet procedures) or soft tissue block (Putti–Platt or Magnuson–Stack procedures) [12].

Worldwide, Bankart repair accounts for almost 90% of primary surgeries for anterior instability. However, in France 72% of surgeons prefer the Latarjet repair as a primary surgery for instability [13].

More specifically, the Bankart repair consists of repairing and reinserting the ligaments in their original position and the Latarjet procedure consists of transferring the coracoid process with the conjoined tendon to fill in the bony defect in the glenoid. The Bankart repair and Latarjet procedure can be performed open, which involves a larger incision and the repair is done under direct visualization, and arthroscopically, which means that the procedure is performed through small incisions while the surgeon sees the inside of a joint using a camera. Besides, there are other surgical techniques such as *remplissage*, humeral osteotomy and humeral head allograft which may be employed to address Hill-Sachs lesions. *Remplissage* has gained popularity in recent years and consists of "filling in" the defect in the humeral head by performing an infraspinatus tenodesis within the defect [6].

Following shoulder surgery, it is recommended for the patients to perform only certain types of activities and to be accompanied by a physical therapist to help restoring the shoulder movement.

The recurrence rate after a primary traumatic anterior dislocation that is treated non-surgically can exceed 70%, while if treated surgically, the rate recurrence has been shown to significantly decrease to 17.5%. This percentage (17.5%) may be a consequence of limited knowledge as to which is the best surgery for each situation. Besides, the Bankart repair has a recurrence rate of about 10%, while the Latarjet technique has a recurrence rate of 5%. However, the performance of the Latarjet procedure should be proposed with caution to patients with a first-time dislocation that present an intact glenoid, as this could lead to greater postoperative pain [12,13].

Furthermore, the study by Itoi *et al*, 00 [21] concluded that a glenoid defect larger than 21% of the glenoid width would limit external rotation after undergoing a Bankart repair. And, according to a study by Boileau *et al*, 06 [50], patients with hyperlaxity and glenoid bone loss that undergo arthroscopic Bankart repair are at risk for recurrent instability.

It has been reported that arthroscopic procedures have 12.6% recurrence, while open procedures show better results with a recurrence rate of 3.4%. Nevertheless, open procedures show certain limitations, such as restrictions on postoperative external rotation and increased postoperative pain. So, a modern arthroscopic stabilization, which repairs with suture anchors, has become the primary surgical option for the management of anterior instability, since it has been shown that this alternative reduces failure rates compared to other arthroscopic techniques, having similar success rates as open stabilization [12].

Some factors increase the risk of persistent instability after surgery, such as suffering trauma, younger age, male gender and participation in contact/collision sports. In addition, some authors have reported that the number of dislocations before the primary surgery may also have an influence. However, a study has shown that if a patient undergoes a Latarjet procedure, the number of dislocations has no influence on the recurrence rate, which means that this is only true when the patient undergoes arthroscopic Bankart repair [13].

Therefore, the physician should have into account the history of the patient, as well as its age and its gender, when deciding on the most appropriate treatment.

The current literature lacks comprehensive comparative studies, due to the variety of surgical treatment techniques available and the heterogeneity among patients. Below, to prove the inaccuracy in the literature, the information found is summarized:

- Glenoid "critical" bone loss should be lower than 20%, since bone loss above 13.5% led to an unacceptable outcome after undergoing Bankart repair [20];
- An osseous defect requires a graft when its width is at least 21% of the glenoid length [21];
- A coracoid transfer is recommended for any defect greater than 25% of the glenoid width, while if the defect is smaller than 25% it is enough to perform a Bankart repair [61];
- Performing a *remplissage* procedure for an engaging Hill-Sachs lesion in the presence of modest glenoid bone loss proved to be a good option [62];
- Lesions with a size of 12.50% of the diameter of the humeral head may have biomechanical implications on glenohumeral joint stability; defect sizes bigger than 37.5% of the diameter of the humeral head can easily lead to shoulder dislocation and in this case it is usually recommended bone grafting [23];
- Hill-Sachs lesions of 5/8 the humeral head radius may require treatment [22];
- Defects on the humeral head greater than 30% should be addressed with an open bone graft or with an arthroscopic remplissage technique [48];
- Glenoid defects smaller than 25% combined with a non-engaging Hill-Sachs lesion should undergo arthroscopic Bankart repair, while if combined with an engaging Hill-Sachs lesion the patient should also be subjected to a *remplissage*; If the glenoid defects are greater than 25% a Latarjet procedure should be performed for a non-engaging Hill-Sachs lesion, and a Latarjet combined with a *remplissage*/bone graft should be performed for an engaging Hill-Sachs lesion [63];
- Defects of 10-20% of the glenoid width combined with defects of 19% of the humeral head diameter cause instability, and therefore at least one of the defects should be addressed with a bony reconstruction [9];
- An open bony procedure should be performed when there is a glenoid bone loss greater than 20 % combined with an engaging Hill-Sachs lesion [48];

Measurement of glenoid bone loss can help the surgeon decide whether bone grafting is required for restoring stability [63]. Thus, it is necessary to obtain an "en face" view of the injured glenoid and compare it with an estimation of the native glenoid. This can be made by: (1) best-fit circle method or (2) comparison with contralateral shoulder. And the measurement of the bone loss can be made through a linear or an area method, as shown in figure 2.17.
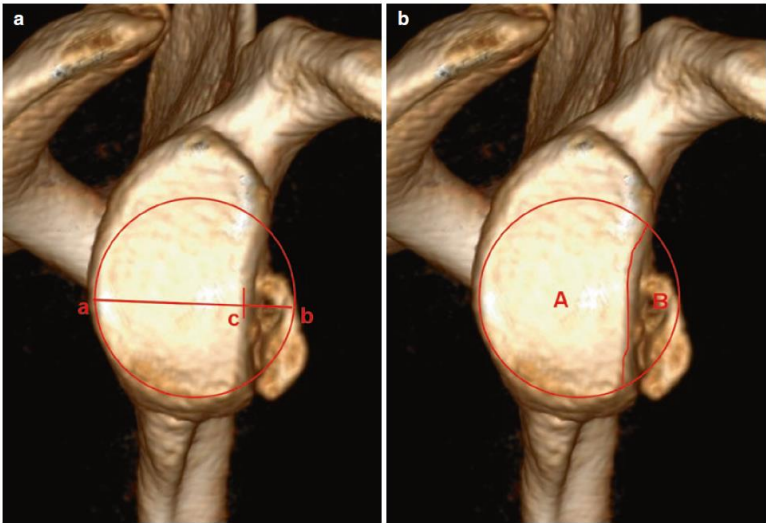
Figure 2.17 – Methods of measuring the glenoid defect (a) linear method and (b) area method [63].

Chapter 3

Finite Element Method

Solids can be subjected to loads or forces, which causes stresses. These stresses lead to deformations or displacements in the solid, which are called strains. Therefore, solving a solid mechanics problem involves dealing with the relationships between stresses and strains, stresses and forces, and displacements and forces, as shown in figure 3.1.
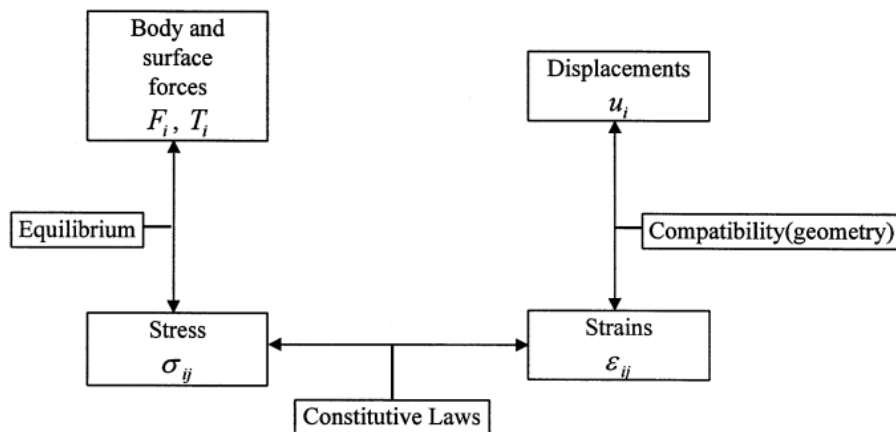
Figure 3.1 -Relationships between variables in solving a solid mechanics problem [64].

Besides, depending on the material properties of the solid, these may have different behaviors when subjected to external forces. Elastic solids return to their original shape when the load is removed (stress-strain relation is reversible), while plastic materials present permanent deformation after the load is removed. Further, the materials can be either isotropic or anisotropic. Materials classified as isotropic will exhibit the same behavior when subjected to a load in any direction. Whereas, anisotropic materials have different behaviors when subjected to loads with the same magnitude, but in different directions [65].

The displacement vector defines the movement of a certain point:

$$\boldsymbol{u} = [u, v, w]^T, \tag{3.1}$$

where u, v, w are the displacements of that point in the directions $x, y, z,$ respectively. The strain vector, which is defined by six strain components, is written as:

$$\varepsilon = \begin{bmatrix} \varepsilon_x \\ \varepsilon_y \\ \varepsilon_z \\ \gamma_{xy} \\ \gamma_{xz} \\ \gamma_{yz} \end{bmatrix} = \begin{bmatrix} \frac{\partial u}{\partial x} \\ \frac{\partial v}{\partial y} \\ \frac{\partial w}{\partial z} \\ \frac{\partial u}{\partial y} + \frac{\partial v}{\partial x} \\ \frac{\partial u}{\partial z} + \frac{\partial w}{\partial x} \\ \frac{\partial v}{\partial z} + \frac{\partial w}{\partial y} \end{bmatrix}, \tag{3.2}$$

where the ε_x, ε_y, ε_z are the normal strains and γ_{xy}, γ_{xz}, γ_{yz} are the shear strains. Thus, the strain vector can also be expressed as:

$$\varepsilon = L\boldsymbol{u}, \tag{3.3}$$

where L is a matrix of partial differential operators and $\boldsymbol{u}$ is the displacement vector. Similarly, the stress vector is also defined by six components and is written as:

$$\sigma = \begin{bmatrix} \sigma_x \\ \sigma_y \\ \sigma_z \\ \tau_{xy} \\ \tau_{xz} \\ \tau_{yz} \end{bmatrix}, \tag{3.4}$$

where σ_x, σ_y, σ_z are the normal stresses and τ_{xy}, τ_{xz}, τ_{yz} are the shear stresses, with $\tau_{ij} = \tau_{ji}$.

Constitutive equations establish the relationship between stress and strain. For anisotropic materials, the constitutive equation can be given by:

$$\sigma = c\,\varepsilon, \tag{3.5}$$

where c is a matrix composed by the material constants, obtained through experimental data [65].

For isotropic materials, since it only requires two independent material constants – the Young's modulus (E) and Poisson's ratio (v), the constitutive equation can be reduced to:

$$\sigma = \frac{E}{(1+v)(1-2v)} \begin{bmatrix} 1-v & v & v & 0 & 0 & 0 \\ v & 1-v & v & 0 & 0 & 0 \\ v & v & 1-v & 0 & 0 & 0 \\ 0 & 0 & 0 & 1-2v & 0 & 0 \\ 0 & 0 & 0 & 0 & 1-2v & 0 \\ 0 & 0 & 0 & 0 & 0 & 1-2v \end{bmatrix} \begin{bmatrix} \varepsilon_x \\ \varepsilon_y \\ \varepsilon_z \\ \gamma_{xy} \\ \gamma_{xz} \\ \gamma_{yz} \end{bmatrix} \tag{3.6}$$

The surface tractions are expressed as [66]:

$$\sigma_x n_x + \tau_{xy} n_y + \tau_{xz} n_z = t_x$$
$$\tau_{xy} n_x + \sigma_y n_y + \tau_{yz} n_z = t_y \tag{3.7}$$
$$\tau_{xz} n_x + \tau_{yz} n_y + \sigma_z n_z = t_z$$

Where n_x, n_y and n_z are the unit normal vectors.
The equilibrium equations are defined as:

$$\frac{\partial \sigma_x}{\partial x} + \frac{\partial \tau_{xy}}{\partial y} + \frac{\partial \tau_{xz}}{\partial z} + f_x = 0$$

$$\frac{\partial \tau_{xy}}{\partial x} + \frac{\partial \sigma_y}{\partial y} + \frac{\partial \tau_{yz}}{\partial z} + f_y = 0 \tag{3.8}$$

$$\frac{\partial \tau_{xz}}{\partial x} + \frac{\partial \tau_{yz}}{\partial y} + \frac{\partial \sigma_z}{\partial z} + f_z = 0$$

3.1 – Finite Element Method

The Finite Element Method (FEM) is a numerical method which is used intensively to solve complex engineering problems, as it provides an approximate solution to many problems. Due to the ease of adaptation to biological organisms without invasive intervention, it has become remarkably popular in the biomechanics field [67].

It considers that the region consists of many small and interconnected subregions, which are called elements. These elements are linked by nodes, and this procedure of selecting nodes and forming finite elements is called discretization and it is represented in figure 3.2. For each element we assume an approximate solution and the general equilibrium conditions of the structure are derived [68].
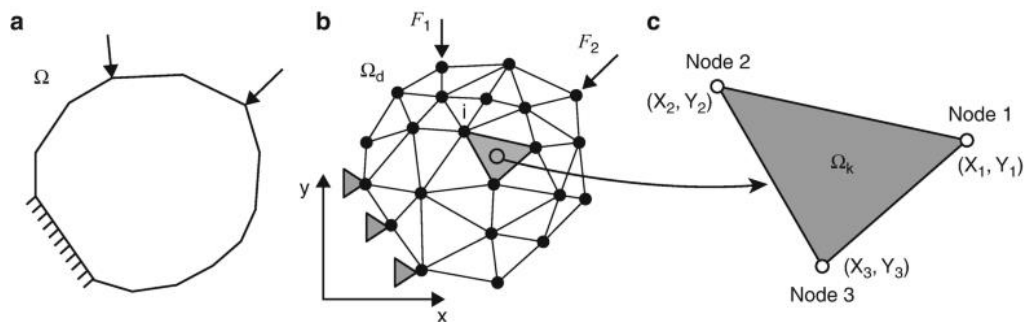
Figure 3.2 – Process of discretization [69].

Consider a triangular finite element that contains a finite size subdomain of the domain in question. The vertices of the triangular element are designated by nodes, which are points in the domain in which the field variable(s) will be calculated explicitly by the FEM.

Since the values of the field variables are obtained explicitly only at the nodes, distributions at the remaining points of an element are obtained by approximating the values obtained at the nodes by means of interpolation functions (usually polynomial functions). For this case:

$$\phi(x, y) = N_1(x, y)\phi_1 + N_2(x, y)\phi_2 + N_3(x, y)\phi_3, \qquad (3.9)$$

where ϕ_1, ϕ_2, ϕ_3 are the values of the field variables in the three nodes and N_1, N_2, N_3 are the interpolation functions.

The following table outlines the steps of the Finite Element Method Analysis:

Table 3.1 — Steps of the Finite Element Method Analysis. Adapted from [68].

Pre-processing	**1.** Discretization of the domain into a set of finite elements: - Definition of the number, type and size of the elements to be used; - Definiton of the connectivity between elements by nodal points located at their boundaries; **2.** Definition of material properties of the elements; **3.** Definition of the boundary conditions; 4. Load application;
Obtaining the solution	5. Choose a set of functions to define the displacement ($\boldsymbol{u}$) within each finite element in terms of their nodal displacements; 6. Calculation, for each element, of the stiffness matrix (k) and the nodal load vector (f); 7. Assembly of the element equations in order to obtain structural equations; $$[k]\{\boldsymbol{u}\} = \{F\}$$
Pos-processing	8. Analyze the structure displacements, strains and stresses.

Chapter 4

Biomechanical modeling

Computer modelling has some advantages that differentiate it from cadaveric studies, such as reproducibility, a range of editable input parameters, output results that may not be possible to obtain through experimental measurements and unlimited testing (for the same model).

Therefore, in order to determine the effect of bipolar lesions in shoulder stability, a finite element model was created.

This model includes the humerus, the scapula and their respective cartilages as done by Walia *et al*, 15 [24]. Besides, it was added the synovial liquid and the glenohumeral capsule.

It is assumed that the model reproduces the reality in order to obtain reliable results.

4.1 – Modeling of the osseous structures

4.1.1 – Mimics

From a set of medical images obtained from CT (computerized tomography), that were used for previous studies [70], 3D models of the humerus and the scapula were created, using the Mimics software (v20). Tools such as Boolean and morphology operations were used to select the two bones and remove some noise. Besides, the "Smooth" tool was also used to smooth the surfaces and the "Wrap" tool to remove small holes. The final model obtained from Mimics is represented in figure 4.1.
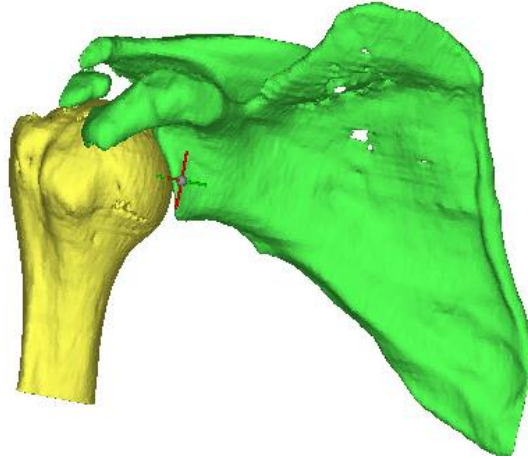
Figure 4.1 – Model obtained from the Mimics software.

4.1.2 – 3-Matic

The model was imported into the 3-Matic software (v12) in order to create the mesh. Besides, some defects (which can be seen in figure 4.1) were corrected and undesirable inner parts were deleted.

It is known that as the size of finite elements tends to zero, the solution obtained converges to the exact solution. However, in order not to get too heavy files, a mesh with triangles with sides measuring approximately 2,5 mm was created. The surfaces of the glenoid and humeral head that will have contact conditions have been assigned with a more refined mesh, as shown in table 4.1. The final model obtained from 3-Matic is represented in figure 4.2.

The files were exported using the .stl format. This format describes unstructured surfaces whose geometric unit of repetition is the triangle, and these are joined by their normal and their vertices using a three-dimensional system of Cartesian coordinates.

Table 4.1— Size of the elements used in the model.

	Humerus	Scapula
General	2,3 mm	2,8 mm
Contact Surfaces	1,4 mm	1,4 mm
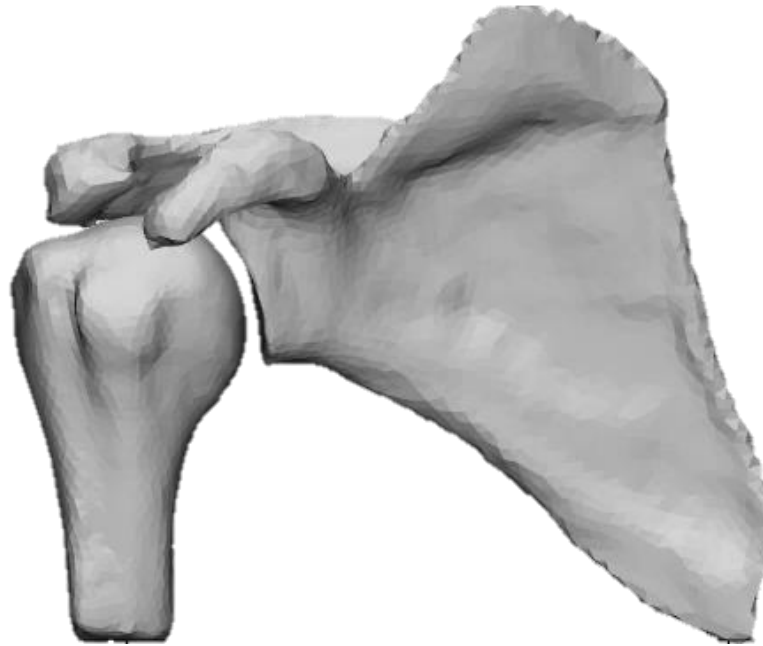
Figure 4.2 – Model obtained from the 3-Matic software.

4.2 - Modeling of the articular cartilages and the glenohumeral capsule

Since the previous model only includes the bony structures, it was necessary to model both the articular cartilages and the glenohumeral capsule.

4.2.1 - Femap

The finite element model was imported into Femap (v11.4.1). In this software the articular cartilages were modeled. The main function of cartilage is to reduce friction and promote good contact between the bones.

So, the elements in the contact areas were extruded in order to represent the cartilage. The placement of the cartilages was not done precisely [33] and there was only a concern to cover the surfaces that, in normal situation, are in contact. The extruded elements are shown in figure 4.3.

In the humerus, the cartilage is thicker at the center and thinner at its periphery, while in the glenoid, the opposite is true. This feature favors the fitting of the humerus in the glenoid and increase the stability of the shoulder complex.

Cartilage was created as having a thickness of 1.5 mm, however since this thickness is not uniform along the surfaces, the simulations will begin by promoting the fit between the surfaces of the humeral head and the glenoid.
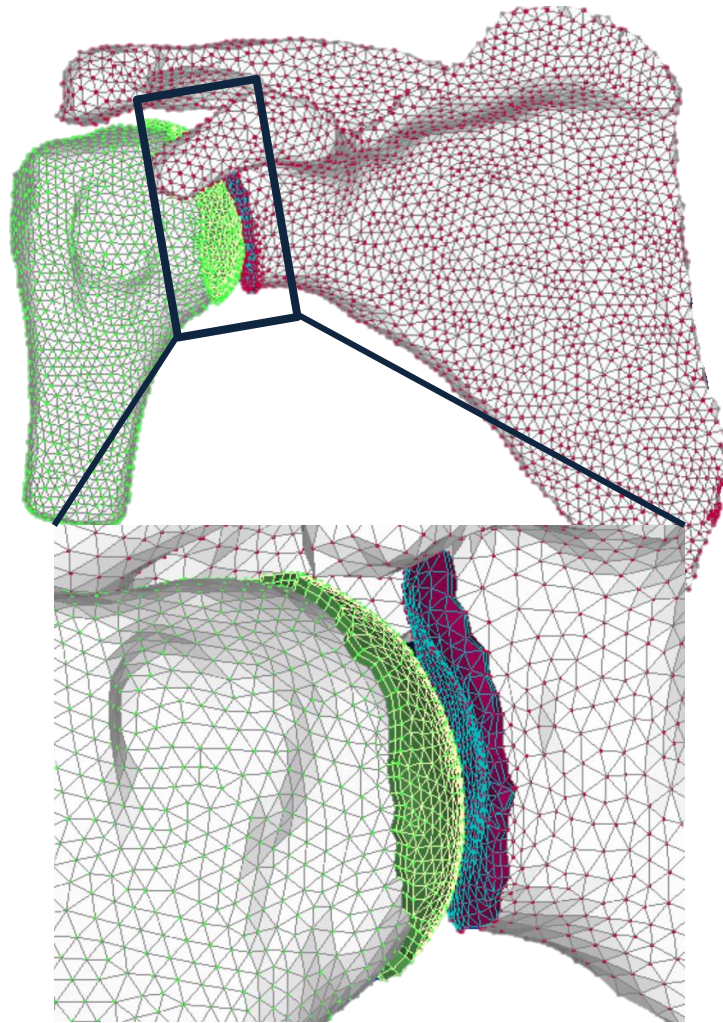
Figure 4.3 – Model obtained from the Femap software, where the colored elements represent the articular cartilages.

4.2.2 - SolidWorks

Solidworks was used to construct the structure of the glenohumeral capsule.

According to literature, it is more appropriate to consider the capsule as a continuous sheet, instead of several discrete structures [18, 71]. Besides, Moore *et al*, 10 [72] showed that modelling the capsule into discrete capsular regions alters the interactions between these regions. More specifically, the results from the study showed that for a discrete model, the average difference between predicted and experimental strains was 20%, while for a continuous model the average difference was 5%.

Therefore, the capsule was modelled as a continuous sheet, as shown in figure 4.4.

Figure 4.4 – Model including the glenohumeral ligaments.

4.3 – Abaqus

The mesh of the capsule was created in Abaqus (2019). Hexahedral elements were used to facilitate the definition of fiber orientation.

As shown in figure 4.5 (a), the posterior section has only one layer (red) since it is thinner, and the section of the capsule which is reinforced by the ligaments has two layers (red and blue).

After the mesh was ready, pressure was applied to the inferior section of the capsule to recreate the insertion of the IGHL into the anatomical neck of the humerus in a U- or V- shape (as shown in figure 4.5 (b)).
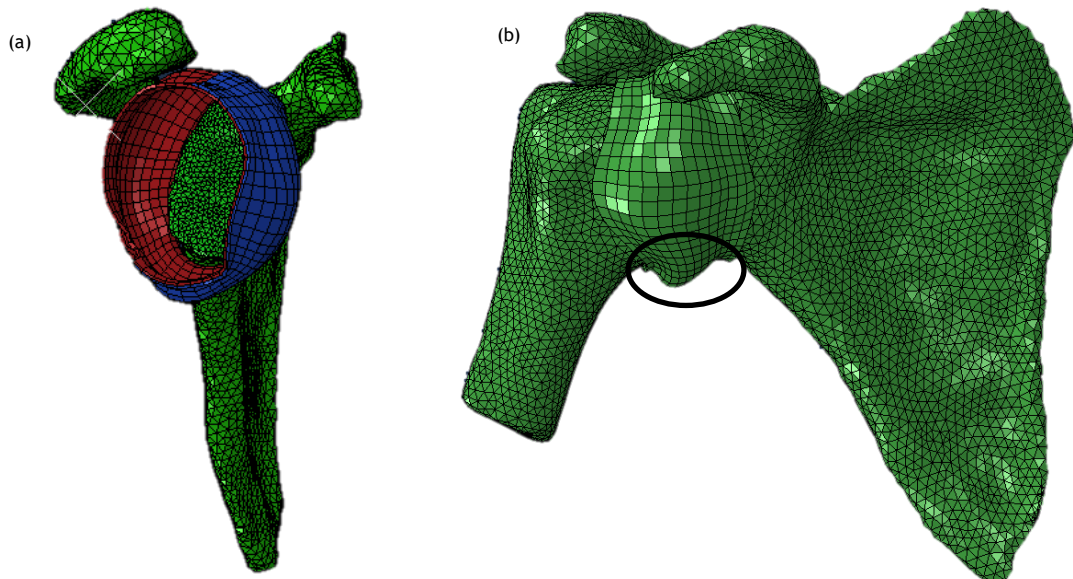
Figure 4.5 – Glenohumeral capsule: (a) lateral view (b) anterior view.

Then, simulations were run in Abaqus to place the bones in the positions of interest, namely:
- 45º of abduction and neutral rotation of the humerus;
- 90º of abduction and neutral rotation of the humerus;
- 45º of abduction and 40º of external rotation of the humerus;
- 90º of abduction and 40º of external rotation of the humerus;
- 45º of abduction and 60º of external rotation of the humerus;
- 90º of abduction and 60º of external rotation of the humerus;

These positions (which are represented in figure 4.6) were chosen since they are related to the position that usually leads to dislocation.

The abduction was performed according to a 2:1 ratio of the glenohumeral and scapulothoracic joints [33], which means that for a total abduction of 45º the glenohumeral joint was abducted 30º and the scapulothoracic joint was abducted 15º and for a total abduction of 90º the glenohumeral joint was abducted 60º and the scapulothoracic joint was abducted 30º.

The external rotation of the humerus was performed by rotating it around an axis parallel to the main axis of the humerus.
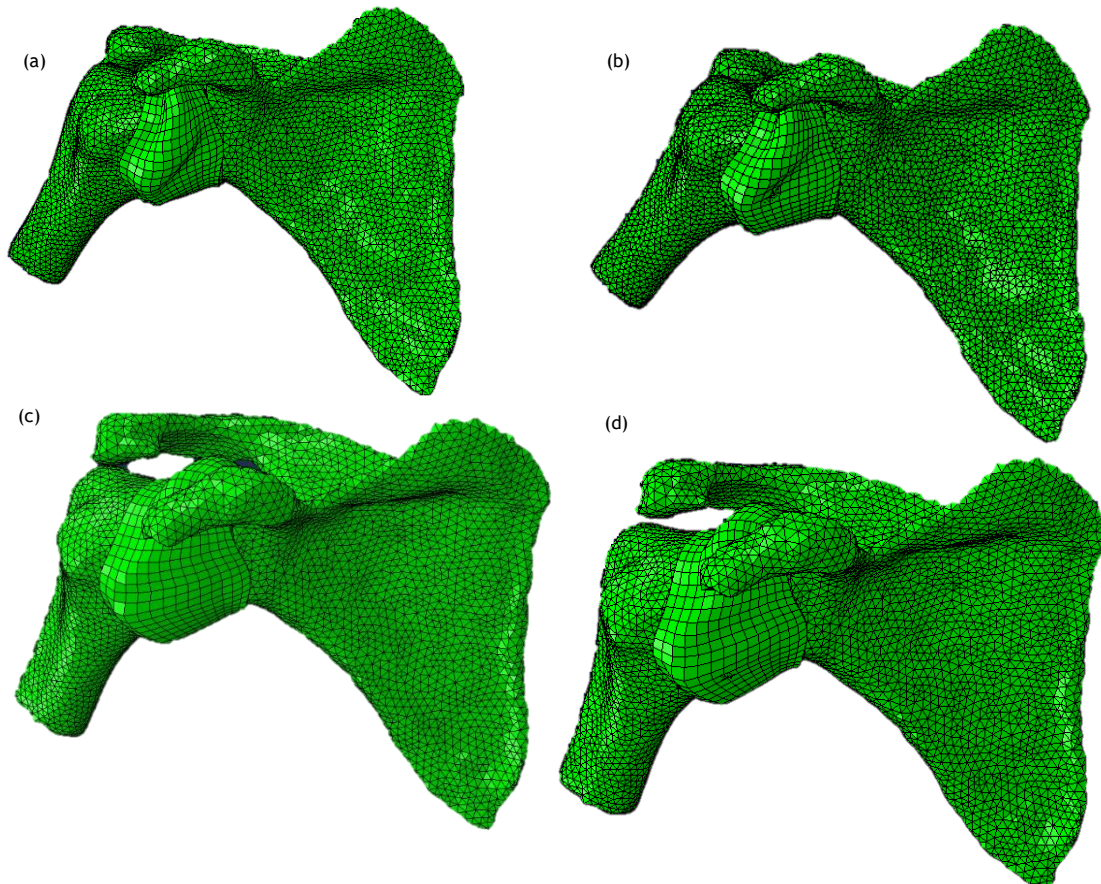
Figure 4.6 – Positions of the humerus (a) 45º of abduction; (b) 90º of abduction; (c) 90º of abduction and 40º of external rotation; (d) 90º of abduction and 60º of external rotation.

4.4 – Creation of defects

In order to study the instability of the shoulder when presenting bipolar lesions (Bankart lesion combined with Hill-Sachs lesion), the influence of defects with different sizes was analyzed. Defects sizes were chosen based on the study by Gottschalk *et al,* 16 [9] for the humeral head and Itoi *et al*, 00 [21] for the glenoid, and are shown in table 4.3.

Table 4.2— Sizes of the defects.

	Humerus (% of the diameter of the humeral head)	**Glenoid** (% of the glenoid width)
Defect 1	2,38 mm (6%)	4,34 mm (12,5%)
Defect 2	7,53 mm (19%)	8,68 mm (25%)
Defect 3	12,28 mm (31%)	13,02 mm (37,5%)
Defect 4	17,43 mm (44%)	17,36 mm (50%)

For the humeral defects, the central point was chosen as the point that was 209º from the anterior border of the humeral head articular cartilage, with the humeral head viewed superiorly, as described by Kaar *et al*, 10 [22]. While for the glenoid defects, it was simulated an oblique osteotomy from the mid-glenoid notch to the 6-o'clock position, as described by Itoi et al, 00 [21]. The defects made are shown in figure 4.7.

Figure 4.7 – (a) Bankart and Hill-Sachs defects created in this work; (b) Osteotomy cut lines adapted from [21,22].

4.5 – Materials Properties

Recreating the behavior of biological materials proved to be quite challenging. However, there are already some cases in the literature in which the behavior of the bones and articular cartilage that make up the shoulder has been recreated and whose approaches have been validated.
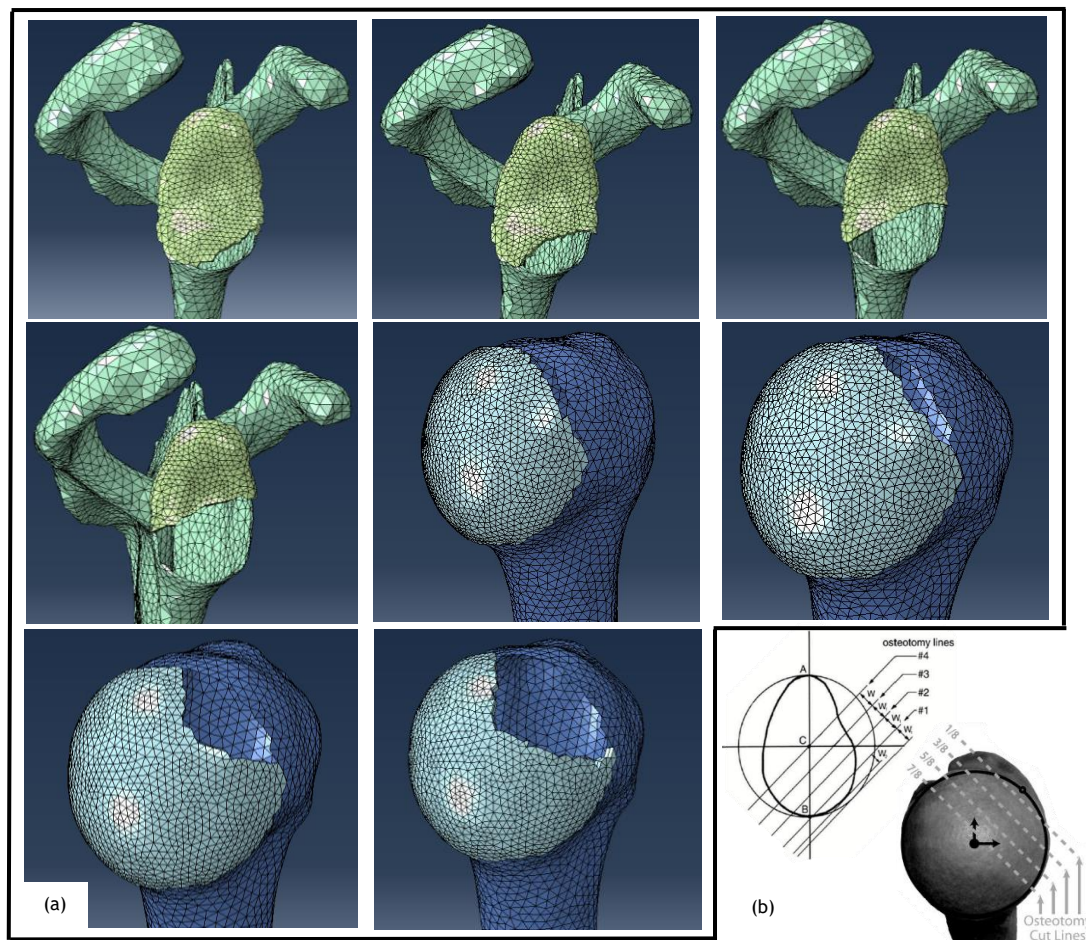
Therefore, for this work, bones were assumed to be rigid bodies as bone deformation is almost negligible when compared to soft tissues and to reduce computational cost. The articular cartilages were modelled as Neo-Hookean hyperelastic, incompressible material [18,24].

To study the behavior of glenohumeral capsule and ligaments, and following the suggestions of previous studies [72, 73], a hyperelastic constitutive model - Holzapfel-Gasser-Ogden (HGO) - was used. Besides, it was added a numerical damage parameter in order to represent the behavior of the ligaments more accurately. It should be noted that the viscoelastic properties of the ligaments were neglected due to the high viscoelastic time constant of the ligaments when compared to the loading time of interest in this work [73].

Before describing the hyperelastic models that were used, some concepts of continuum mechanics must be introduced.

As previously mentioned, a deformation occurs when a particle is subjected to a load. Therefore, following standard notational convention, it is considered X as the particle's position in the reference configuration Ω_0, whereas x represents the position of the particle in the deformed configuration Ω [74].

The deformation gradient, describes the kinematics of deformation at each point and can be represented by:

$$F(X) = \frac{\partial x}{\partial X} \tag{4.1}$$

The Jacobian of the deformation is the ratio of the reference volume over the deformed volume for a homogeneous deformation at a given point, and is written as:

$$J = \det F = \frac{\rho_0}{\rho}, \tag{4.2}$$

where ρ_0, ρ are the reference and current material densities, respectively. In case the material is incompressible then $J = 1$.

The right and left Cauchy-Green deformation tensors form the basis of constitutive model development for soft tissues, providing deformation measures. These are expressed, respectively, as:

$$C = F^T F \text{ and } B = FF^T \tag{4.3}$$

In order to define the strain, several strain stensors can be used [75].

The Lagrange strain tensor is given by:

$$E = \frac{1}{2}(\boldsymbol{F}^T.\boldsymbol{F} - I) = \frac{1}{2}(C - I),\tag{4.4}$$

where I is the identity matrix. This strain tensor is used when it is expected large deformations.

The Eulerian strain tensor is very similar to the Lagrange strain tensor. The main difference between these two is that from the orientation after deformation of an infinitesimal line element the Eulerian strain tensor enables to compute the strain. Thus, this tensor is expressed as:

$$E^* = \frac{1}{2}(I - \boldsymbol{F}^{-T}.\boldsymbol{F}^{-1})\tag{4.5}$$

Regarding stress, the first and second Piola-Kirchoff stress tensors are used when stress is referred to the reference configuration and are defined respectively as:

$$P = J\boldsymbol{F}^{-1}\,T,\tag{4.6}$$

$$S = J\boldsymbol{F}^{-1}\,T\,\boldsymbol{F}^{-T} = P\,\boldsymbol{F}^{-T},\tag{4.7}$$

where T is the Cauchy stress, defined as the force acting on the deformed configuration. Thus, the first Piola-Kirchoff stress tensor P refers to the force in the deformed configuration on a surface normal to the axes in the undeformed configuration. Its components can be measured experimentally; however, it is not symmetric. While the second Piola-Kirchoff stress tensor S is symmetric which makes it more commonly used.

For large deformation the tensors S (second Piola-Kirchoff stress tensor) and E (Lagrange strain tensor) frequently appear together in constitutive models.

4.5.1 – Hyperelastic Materials

Hyperelastic materials are a subgroup within elastic materials, in which the stress at each moment in time depends only on the strain on that same moment and does not take into account the history of the strain. The scalar function that describes the hyperelastic materials, from which the stress can be derived at any point $\boldsymbol{X}$ is the strain energy density function (SEDF) and it can be defined in terms of the deformation gradient:

$$\Psi = \Psi(\boldsymbol{F})\tag{4.8}$$

This function must obey the Principle of material frame indifference, which states that under changes of reference frame the constitutive equations must be invariant. Therefore, it may be defined as:

$$\Psi = \Psi(C) \tag{4.9}$$

The way the strain energy depends on C will be restricted by material symmetries. So, if the material is isotropic, Ψ can be expressed through the three principal strain invariants of C.

$$\Psi = \Psi(I_1, I_2, I_3) \tag{4.10}$$

where

$$I_1 = \text{tr}(C) = \lambda_1^2 + \lambda_2^2 + \lambda_3^2 \tag{4.11}$$

$$I_2 = \frac{1}{2}[(\text{tr}(C))^2 - \text{tr}(C^2)] \tag{4.12}$$

$$I_3 = \det(C) \tag{4.13}$$

4.5.1.1 – Neo-Hookean Constitutive Model

In this formulation, the strain energy per unit of reference volume is defined as [76]:

$$\Psi = C_{10}(\bar{I}_1 - 3) + \frac{1}{D_1}(J - 1)^2 \tag{4.14}$$

where C_{10} and D_1 are temperature-dependent material parameters. By setting D_1 to a small value, the material is modeled as incompressible.

J is the elastic volume ratio and $\bar{I}_1$ is expressed as:

$$\bar{I}_1 = J^{-2/3}I_1 \tag{4.15}$$

4.5.1.2 – Holzapfel-Gasser-Odgen Constitutive Model

The HGO constitutive model describes the anisotropic hyperelastic behavior of collagen fiber-reinforced biological materials.

In the HGO model the deformation gradient is given by:

$$\boldsymbol{F} = \left(J^{1/3}I\right)\bar{F}, \tag{4.16}$$

where I is the identity tensor. The $J^{1/3}I$ is the volumetric part and $\bar{F}$ the isochoric part ($\det \bar{F} = 1$).

The right Cauchy-Green deformation tensor is given by:

$$\bar{C} = \bar{F}^T \bar{F} = J^{2/3} C \tag{4.17}$$

In this model, the strain energy density function is defined as:

$$\Psi = \Psi_{vol} + \Psi_{mat} + \Psi_{fib}, \tag{4.18}$$

where Ψ_{mat} corresponds to the contribution of the matrix, Ψ_{fib} corresponds to the contribution of the fibers and Ψ_{vol} enables the compressible behavior of the material.

$\Psi_{vol}, \Psi_{mat}, \Psi_{fib}$ are expressed as:

$$\Psi_{vol} = \frac{1}{D}\left(\frac{\left(J^{el}\right)^2 - 1}{2} - \ln J^{el}\right) \tag{4.19}$$

$$\Psi_{mat} = C_{10}(\bar{I}_1 - 3) \tag{4.20}$$

$$\Psi_{fib} = \frac{k_1}{2k_2}\sum_{\alpha=1}^{N}\{\exp[k_2\langle\bar{E}_\alpha\rangle^2] - 1\} \tag{4.21}$$

with

$$\bar{E}_\alpha = k(\bar{I}_1 - 3) + (1 - 3k)\left(\bar{I}_{4(\alpha\alpha)} - 1\right), \tag{4.22}$$

where C_{10}, D, k_1 and k_2 are material coefficients.

N is the number of fiber families, which we assumed in this work to be $N = 1$, and k is a parameter that controls the dispersion of the fibers around the mean direction (it can have a value between 0 and 1/3 - if k =0 it means the fibers are perfectly aligned in the preferencial direction, whereas if k =1/3 it means that the fibers are randomly distributed).

$\bar{I}_1$ is the first strain invariant and $\bar{I}_{4(\alpha\alpha)}$ are pseudo-invariants of the deviatoric part of the right Cauchy-Green deformation tensor.

$$\bar{I}_1 = J^{-2/3}I_1 \tag{4.23}$$

$$I_4 = a_0\,(Ca_0) \tag{4.24}$$

$$\bar{I}_4 = J^{-2/3}I_4 \tag{4.25}$$

where a_0 is a unit vector that represents the direction of the fiber in the reference configuration.

To define the preferential direction of the fibers it was adapted a Matlab routine from [77]. This created a vector at the centroid of each element defining the orientation of the fibers, as shown in the following figure.
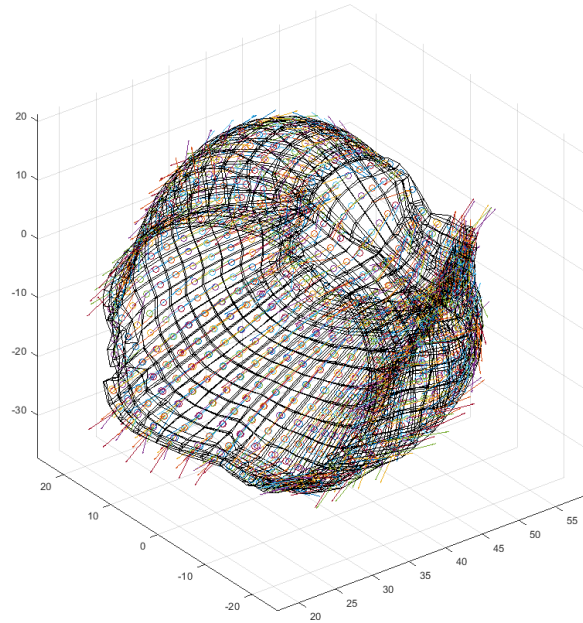

Figure 4.8 – Output from the Matlab routine.

4.5.2 – Anisotropic damage at finite strains

Experimental data shows that when tissues undergo axial tensile stresses, their response is typically non-linear.

The HGO constitutive model, despite describing the material properties of the ligaments, is limited to the range of physiological loads. Therefore, in order to represent the ligaments more accurately, it should be considered the non-physiological loads, which cause soft tissues to damage arising from the tear or plastic deformation of the fibers.

So, a model that describes the reduction in the mechanical stiffness of ligaments when non-physiological strains lead to progressive failure of the fibers was used [78]:

$$\Psi = \Psi_{vol} + (1 - D_m)\Psi_{mat} + \left(1 - D_f\right)\Psi_{fib}, \tag{4.26}$$

where $D_m \, \epsilon \, [0,1]$ is the damage variable for the matrix and $D_f \, \epsilon \, [0,1]$ is the damage variable for the fibers. $(1 - D_m)$ and $\left(1 - D_f\right)$ are known as reduction factors.

The damage function is expressed as:

$$g = \begin{cases} 1 & if & \Xi_t < \psi_{min} \\ \dfrac{1 - e^{\beta(\Xi_t - \psi_{max})}}{1 - e^{\beta(\psi_{min} - \psi_{max})}} & if & \psi_{min} \leq \Xi_t \leq \psi_{max} \\ 0 & if & \Xi_t > \psi_{max} \end{cases} \tag{4.27}$$

where ψ_{min} is the strain energy at initial damage, ψ_{max} is the strain energy at total damage and β is an exponential parameter.

In order to implement the material properties, a user-defined material (UMAT) subroutine was executed, based on the subroutine developed by Ferreira *et al*, 17 [79].

Thus, the parameters used are shown in Table 4.3.

The elements that make up the cartilage and the ligaments have been modified to hybrid elements, C3D6H and C3D8H, respectively. These are used to model incompressible materials (or nearly incompressible).

Table 4.3 — Material properties.

	Type	Parameters	Number of elements (Element type)
Humerus	Rigid body	-	5662 (S4R)
Scapula	Rigid body	-	19775 (S4R)
Articular cartilage	Hyper-elasticity	$C_{10} \approx 1.79$ MPa	5650 (C3D6H)
Glenohumeral capsule	Hyper-elasticity	$C_{10} = 3.82^{-1}$ MPa $k_1 = 1^{-4}$ MPa $k_2 = 5^{-3}$ $k = 5^{-3}$ $\psi_{max}^f = 3.15^{-1} \sqrt{\text{MPa}}$ $\psi_{min}^f = 5^{-4} \sqrt{\text{MPa}}$	1048(C3D8H)

It should be noted that no sections were considered to define the properties of the glenohumeral capsule and ligaments, since it was reported that the differences between these were minimal [81].

4.6 – Glenohumeral capsule parameters

In order to establish the parameters that would allow to recreate the behavior of the capsule, it was used a cube to reduce the computational cost. Several parameters were tested so that the output was as similar as possible to the stress-stretch curve in the literature.
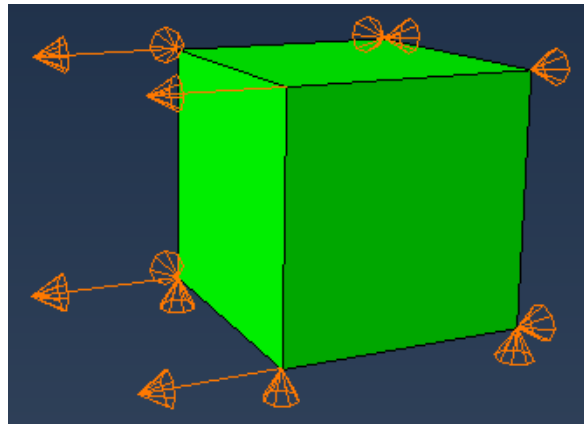
Figure 4.9 – Conditions applied to the cube.

The parameters used are shown in table 4.3 and the following figure shows a graph with the stress-stretch curve in the study by [46] and the curve obtained in this work. It is important to note that the graph from the literature consists of an average of the values obtained for all the tested sections of the injured capsule.
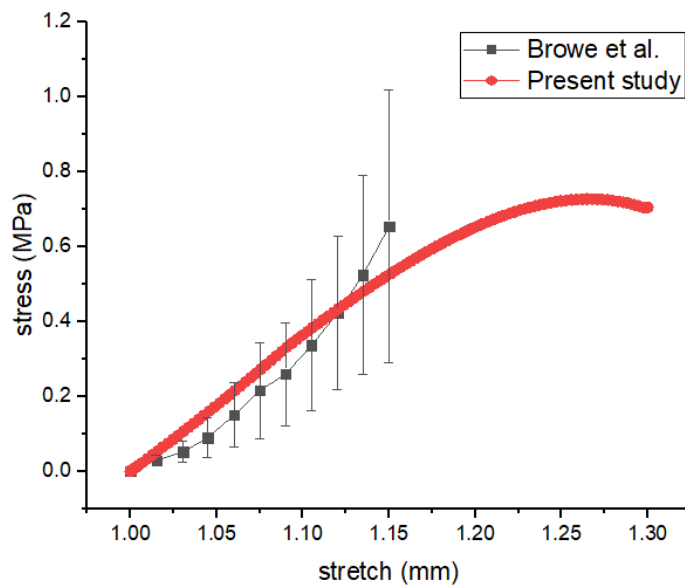
Figure 4.10 – Stress-stretch curve from [46] and from this work.

4.7 – Simulations

4.7.1 – Conditions

The interaction between the cartilage of the glenoid and the cartilage of the humerus was defined as frictionless with a tangential behavior using a surface-to-surface formulation [33].

A contact between the bone surfaces and the capsule was also defined to prevent the capsule from penetrating the bones.

Moreover, the capsule was tied to the bones so that it could follow the motion of the bones.

Finally, a fluid cavity was created to simulate the effect of synovial fluid. A density similar to that of water was considered, which is approximately 1^{-09} ton/mm^3.

The coordinate system used is shown in figure 4.9.
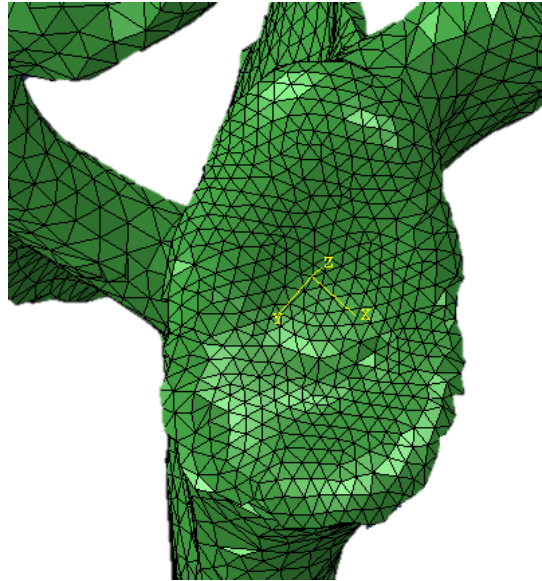
Figure 4.11 – Coordinate system used.

4.7.2 - Steps
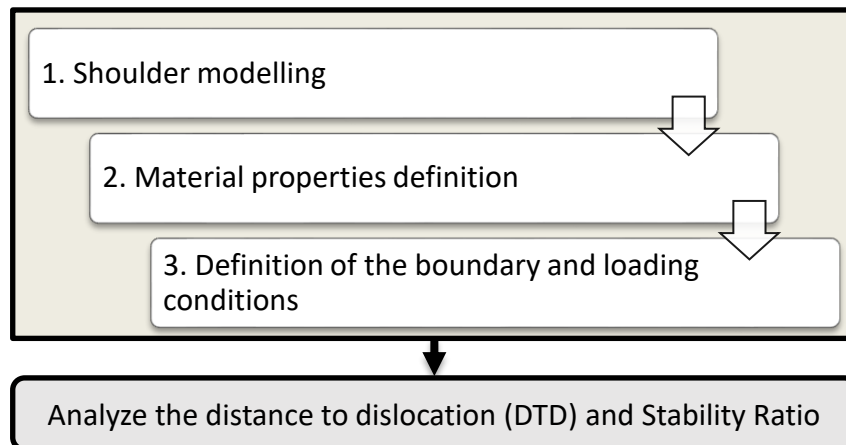
Figure 4.12 – Block diagram of the method used.

Simulations were run in the presence of bipolar lesions to analyze the DTD (distance to dislocation) and the Stability Ratio. These comprised 3 steps: pre-tension, contact and translation.

Since the capsule only acts as a stabilizer of the glenohumeral joint when it is under tension [21], pre-tension step consisted of ensuring this. In the initial position the cartilages are inside each other, and with the stretching of the capsule, the cartilages separate, creating tension in the capsule. Figure 4.11 shows the initial and final positions of the cartilages during this step.

Then, the contact between the two cartilages was promoted, moving the humerus in the medial direction and restricting all other movements.

In the final step, the humeral head was translated in the antero-inferior direction (x-axis), and rotation was restricted in all axis. During all the steps of the simulation the scapula was considered static.

(a)

(b)
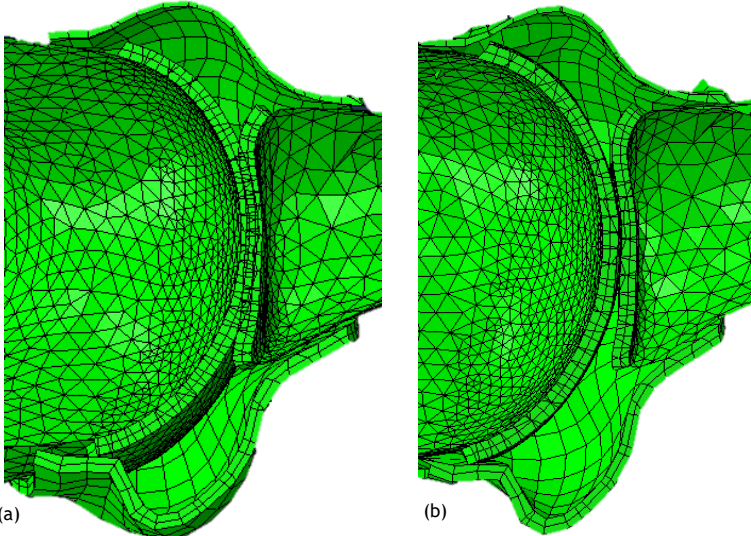
Figure 4.13 – (a) Initial and (b) final positions of the cartilages during pre-tension step.

Chapter 5

Results & Discussion

In order to conclude regarding the defects sizes that lead to shoulder dislocation, the distance to dislocation (DTD) and the Stability Ratio were evaluated, as previously done in other studies [9,24].

Since a damage parameter was added to define the material properties, it was analyzed the sections where the damage was higher. The output obtained is in accordance with the literature since the damage in the IGHL is higher in the glenoid insertion and in the ligament's midsubstance [52], as shown in figure 5.1.
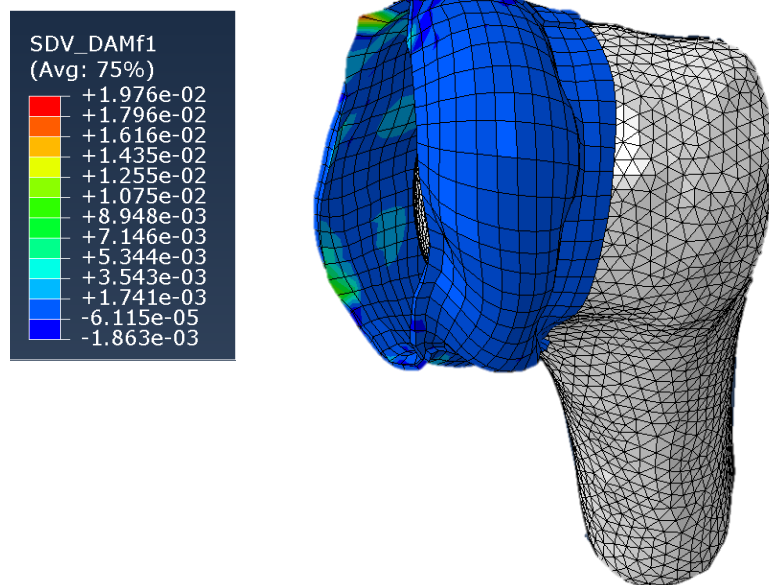
Figure 5.1 – The damage distribution on the capsule.

Due to the lack of elements in the defects, when the humerus translates in the anterior-inferior direction, the simulation will stop as soon as the contact between the humeral head and the glenoid is not stable. The distance that the humerus moves before reaching instability is the DTD.

The figures below show the DTD obtained for the different positions tested and with different defects combined.
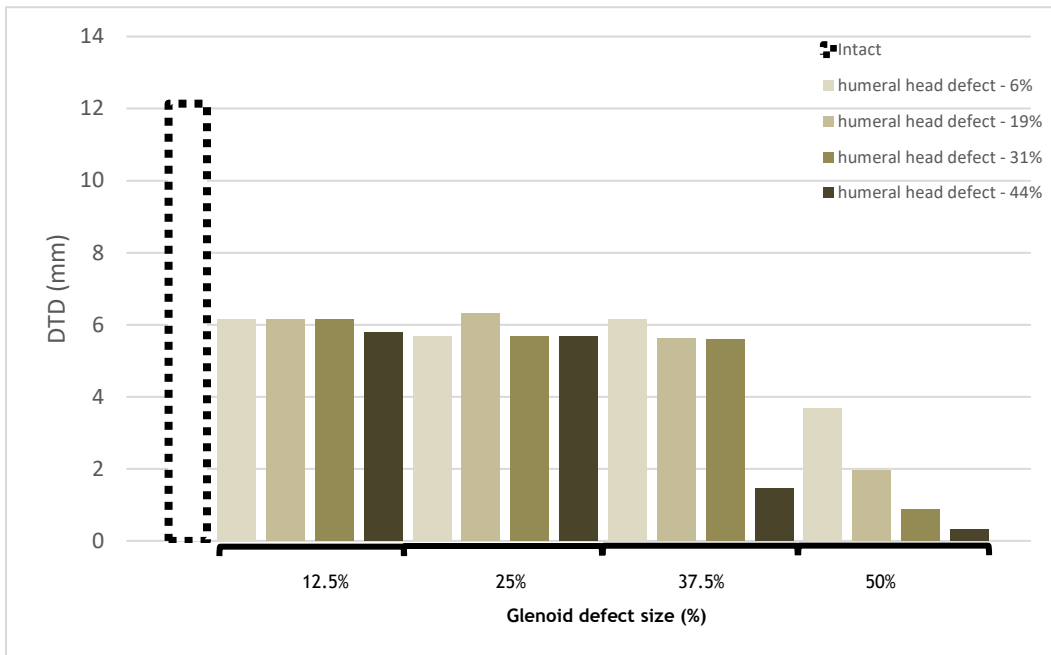
Figure 5.2 – DTD for the different combination of defects for the humerus with 45° of abduction and Neutral Rotation.
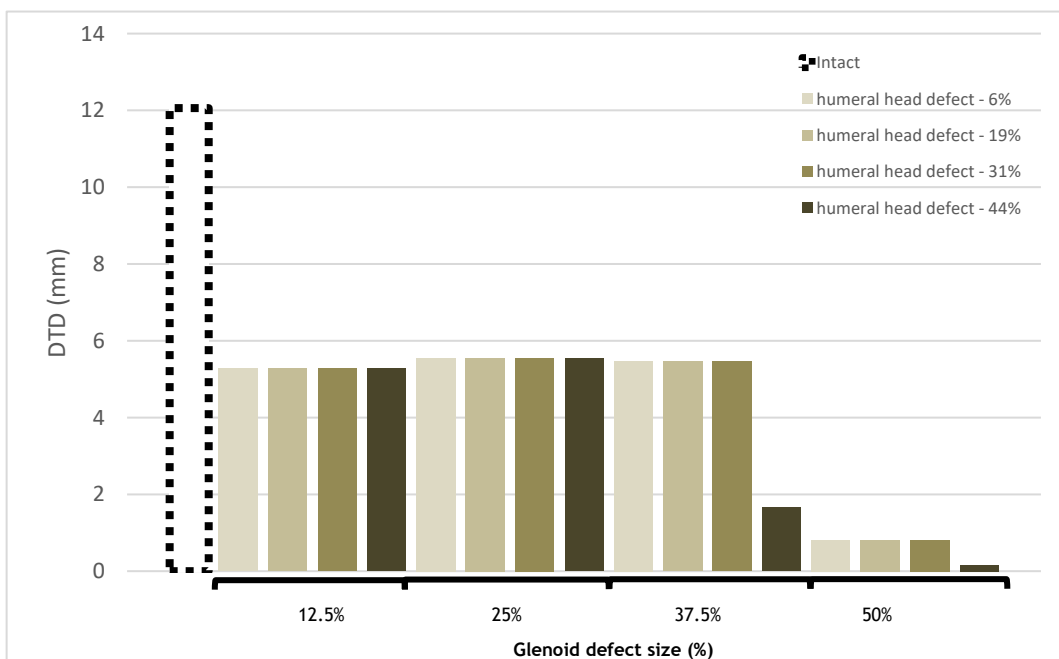
Figure 5.3 – DTD for the different combination of defects for the humerus with 90° of abduction and Neutral Rotation.
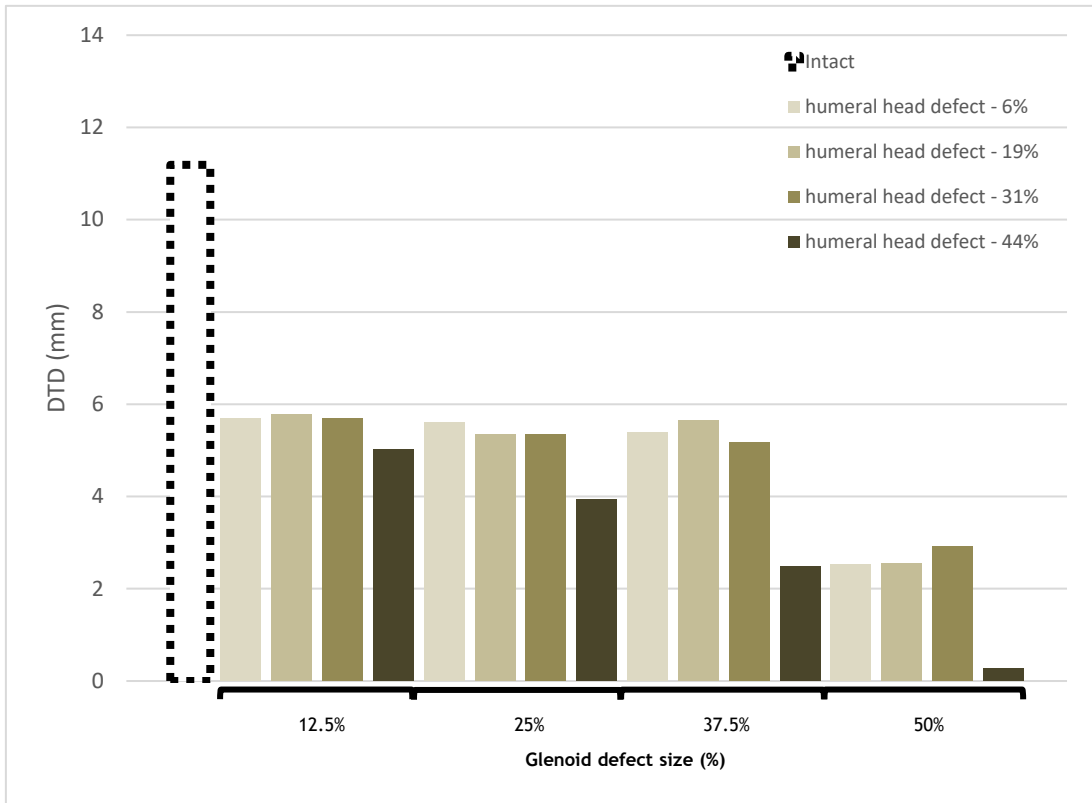
Figure 5.4 - DTD for the different combination of defects for the humerus with 45° abduction and 40° of external rotation.
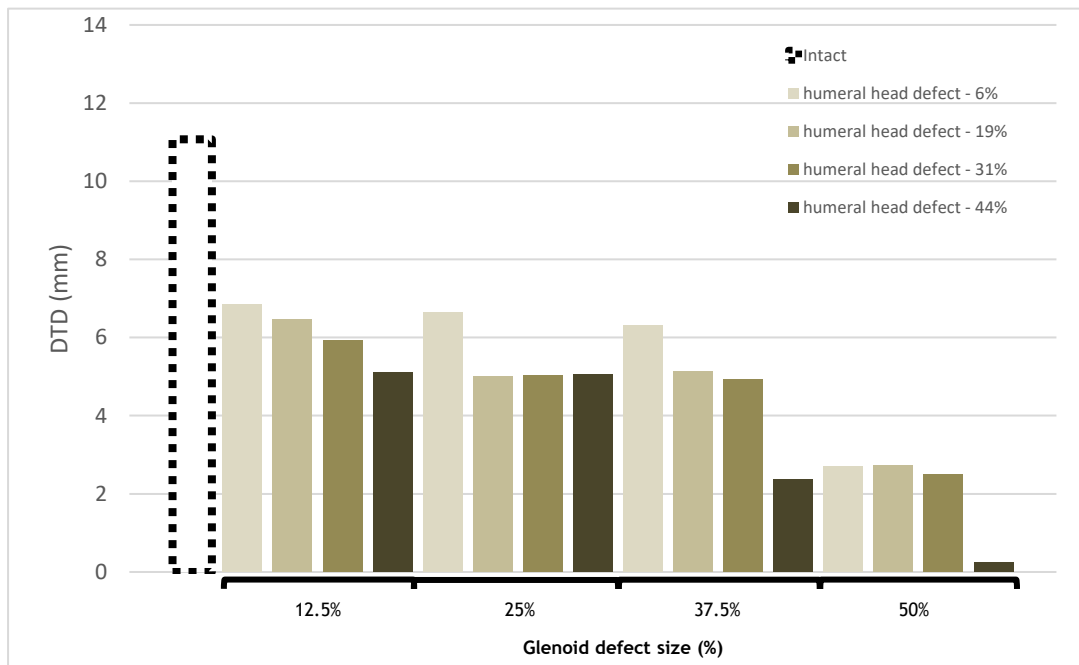
Figure 5.5 - DTD for the different combination of defects for the humerus with 45° abduction and 60° of external rotation.
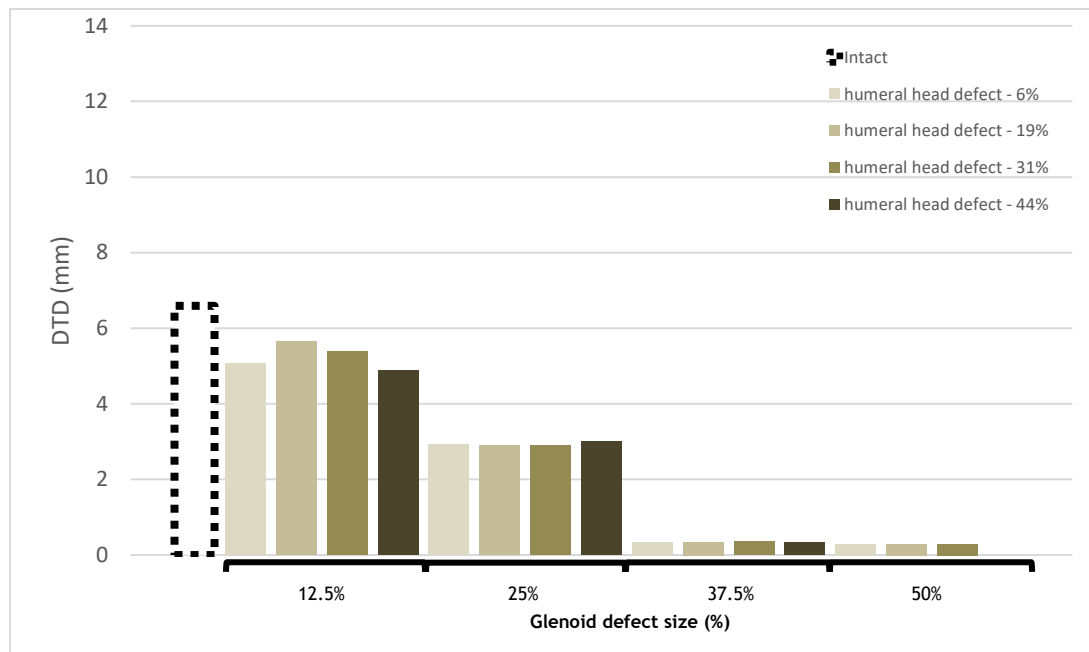
Figure 5.6 – DTD for the different combination of defects for the humerus with 90º abduction and 40º of external rotation.
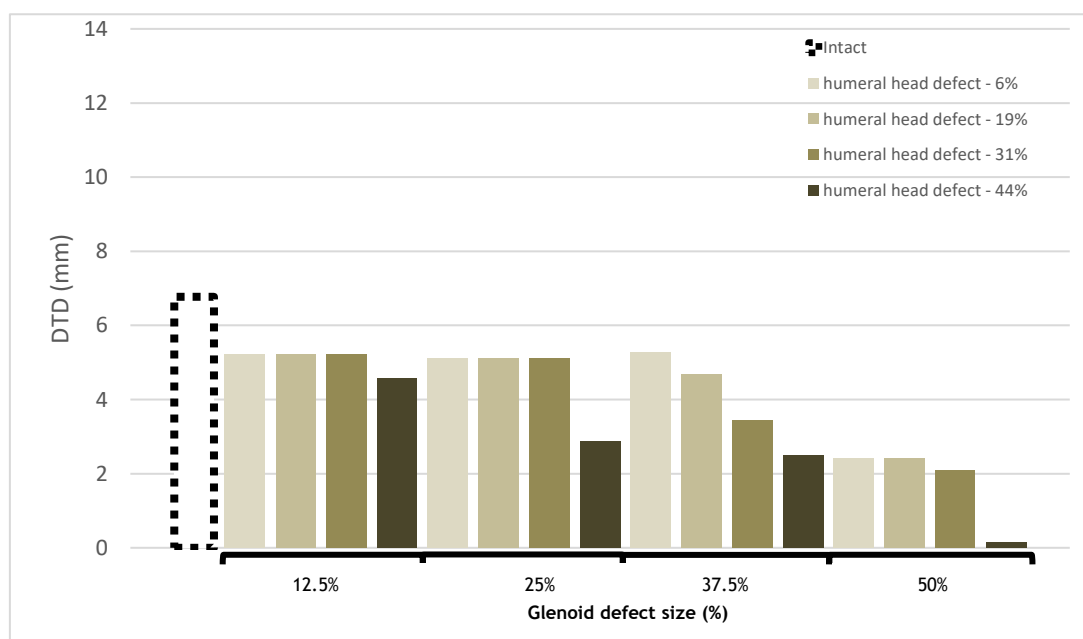
Figure 5.7 – DTD for the different combination of defects for the humerus with 90º abduction and 60º of external rotation.

After analyzing the graphs, one can conclude that the DTD is smaller as the defects become larger, as demonstrated in other studies. In addition, it was also concluded that the distance changes with the different positions of the humerus.

For the humerus abducted 45º/90º and with neutral rotation, the DTD is approximately the same for all sizes of defects, except for the glenoid defect with a size of 50% of the glenoid width combined with any humeral head defect and the glenoid defect of 37.5% combined with

a humeral head defect of 44%. However, the DTD for the humerus with 45° abduction is about 6 mm and for 90° it is about 5 mm. Therefore, it can be concluded that the humerus is more unstable for higher abduction angles.

When the humerus is externally rotated with 45° of abduction, Hill-Sachs defects have a greater influence on the stability as the external rotation angle increases. But, in general, the DTD did not present very distinct differences between the external rotation of 40° and 60°.

Moreover, when the humerus is externally rotated at 90° of abduction, different data were obtained from what is presented in the literature. In other words, the DTD for the humerus externally rotated 60° were bigger from the glenoid defect of 25% of the glenoid width when compared with distances with the humerus rotated 40°. This can be justified by the fact that it was considered the presence of the glenohumeral ligaments, which stabilize the shoulder in upper ranges.

In summary, when the humerus was with neutral rotation, the size of the glenoid defect was the main cause for instability, while the humeral head defects had more influence when the humerus was externally rotated. Therefore, it can be concluded that the glenoid defects lead to translational instability while the humeral head defects lead to rotational defects, as it was also concluded in other study [24].

For all the positions that were tested, the presence of combined defects with the maximum sizes (50% for glenoid and 44% for humeral head) caused the glenohumeral joint to be completely unstable. Besides, the presence of the glenoid defect with a size of 50% of the glenoid width showed small distances to dislocation in all the positions, regardless of the size of the humeral head defect. The glenoid defect of 12.5% and 25% showed similar results for most of the cases. Although these do not easily lead to dislocation, the values obtained were still low compared to the values of an intact glenohumeral joint. The glenoid defect of 37.5% leads to less stability when combined with humeral head defects of 31% and 44%.

Moreover, the influence of the defects on glenohumeral stability not only depends on its size but also on its location. Therefore, it is important to note that if other method was used to create the defects, the results might have been different.

To evaluate the stability of the glenohumeral joint, it was calculated the stability ratio. The stability ratio equation is shown in chapter 2. The compressive force was considered as the force of the humerus against the glenoid during the contact step and the translational force was considered as the force on the humerus that allows its translation in the anterior-inferior direction until a dislocation or subluxation occurs.

The table below shows the stability ratio obtained for each case:

Table 5.1 — Stability Ratio for combined defects at 45° and 90°.

Humeral Head Defects					
Glenoid defects (45°)	Intact	6%	19%	31%	44%
Intact	0.49	-	-	-	-
12.5%	-	0.40	0.40	0.40	0.40
25%	-	0.18	0.18	0.18	0.12
37.5%	-	0.11	0.10	0.08	0.08
50%	-	0.08	0.08	0.05	0
Glenoid defects (90°)	Intact	6%	19%	31%	44%
Intact	0.47	-	-	-	-
12.5%	-	0.26	0.26	0.26	0.26
25%	-	0.14	0.14	0.14	0.13
37.5%	-	0.12	0.12	0.13	0.11
50%	-	0	0	0	0

For a healthy glenohumeral joint, we obtained the ratio of 47% and 49% for the abduction angles of 90° and 45°, respectively. These values are similar to the ratio of 43% and 44% obtained in the study by Walia *et al*, 13 [33].

The stability ratio did not show big differences as the size of the Hill-Sachs defects got bigger.

In addition, these values confirm the fact that the stability of the joint decreases with the increase in the size of the defects.

When the humerus is abducted 45°, the stability ratio showed a biggest decrease with the glenoid defect of 25% of the glenoid width, while for the humerus abducted 90° the biggest decrease was for a glenoid defect of 12.5% of the glenoid width. This information also supports that for larger abduction angles the joint is more unstable.

The outputs from this work allowed us to conclude that glenoid defects with sizes bigger than 37.5% of the glenoid width can easily lead to shoulder dislocation. So, a bone block on the glenoid should be performed to recover the glenohumeral joint stability. For glenoid defects with sizes between 12.5% and 37.5%, a Bankart repair might be able to restore stability. Finally, a *remplissage* might be recommended to address humeral head defects with sizes bigger than 44%, considering the location used in this work.

Chapter 7

Conclusions

The glenohumeral joint is one of the most complex joints, enabling the performance of a wide variety of movements. Given the high mobility of this joint, dislocations are common, especially in the anterior direction. Moreover, a dislocation can lead to the appearance of lesions which in turn increase the likelihood of the patient to have new dislocations. Besides, the inability to choose the most appropriate treatment to treat instability has also proven to contribute to recurrence rates.

Studies have been carried out on this subject, however there is still some inaccuracy in the data available. Therefore, this work aimed to reach to a conclusion regarding the most appropriate treatment for different combinations of lesions with different sizes. A finite element model was built which, in contrast to what exists in the literature, did not neglect the presence of the glenohumeral capsule. Then, the DTD and stability ratio for different positions of the humerus and considering different combinations of defects were analyzed.

It was concluded that the higher the degrees of abduction, the greater the probability of dislocation. In addition, if the humerus also presents external rotation, the probability of dislocation also increases. These results were already expected, based on the results that exist in the literature. However, since this study is the first to consider the presence of the glenohumeral capsule and ligaments, it was found that for an abduction of 90° and with an external rotation of 60°, these played an important stabilizing role. This information confirms that the ligaments are particularly important at upper ranges.

Besides, the results suggested that for glenoid defects between 12.5 - 37.5% of the glenoid width a Bankart repair should be adequate since it allows the recovery of the stabilizing effect of the ligaments. However, for glenoid lesions larger than 37.5%, a Latarjet procedure is recommended.

Humeral head defects with sizes bigger than 44% of the diameter of the humeral head may be addressed with a *remplissage*.

In addition, these conclusions may be important for patients that present these lesions to realize what kind of movements they should avoid (i.e. a patient with a glenoid defect of 37.5% combined with a humeral head defect of 6% should avoid movements such as the abduction of 90° of the arm with external rotation).

It is also important to note that, as in other studies, the creation of the defects took into consideration the same orientation for all the defects, as described in chapter 4. Although this allows reproducibility, it has the limitation of not representing clinical defects.

For future work, it is suggested to add the muscles to the model and evaluate their influence. This, assuming that if the ligaments have been shown to increase stability on upper ranges of abduction, then the muscles may increase stability in the mid- ranges. Besides, the addition of labrum should also contribute to increased stability since it accounts for 10-20% of the stabilizing forces.

Finally, since the lesions are quite varied, it may be interesting to apply this concept to subject-specific models. In other words, through the medical images obtained for a certain patient, transform it into a computational model and understand if it has or not the possibility of recurrence. With this information the physicians can make a much more reasonable decision about whether or not to perform surgery, and if so, if a procedure at the level of soft tissues is enough or if an intervention at the level of bones will be necessary.

References

[1] D. Knudson, *Fundamentals of biomechanics*, Second edition, Springer, 2007.

[2] J. P. Vilas-Boas, Biomecânica do Desporto, Manual de Curso de Treinadores de Desporto, pp. 5-15, 2016.

[3] S. S. Metan, P. Krishna, and G. C. Mohankumar, "FEM Model an Effective Tool to Evaluate Von Mises Stresses in Shoulder Joint and Muscles for Adduction and Abduction." Procedia Materials Science, 5: 2090-2098, 2014.

[4] K. E. Wilk, M. M. Reinold, and J. R. Andrews, "The athlete's shoulder", Philadelphia, PA: Churchill Livingstone/Elsevier, 2009.

[5] C. H. Linaker and K. Walker-Bone, "Shoulder disorders and occupation". Best practice & research, Clinical rheumatology, pp. 405–423, 2015.

[6] M. Varacallo, M. A. Musto, and S. D. Mair, *Anterior Shoulder Instability*. In: StatPearls, Treasure Island (FL): StatPearls Publishing, Jan. 2020.

[7] B. D. Owens, L. Dawson, R. Burks and K. L. Cameron, "Incidence of shoulder dislocation in the United States military: demographic considerations from a high-risk population", The Journal of bone and joint surgery, American volume, 91(4), pp. 791–796, 2009.

[8] J. Chorley, R. Eccles and A. Scurfield, "Care of Shoulder Pain in the Overhead Athlete", Pediatric Annals, 46: 112-113, 2017.

[9] L. J. Gottschalk 4th, P. Walia, R. M. Patel, M. Kuklis, M. H. Jones, S. D. Fening and A. Miniaci, "Stability of the Glenohumeral Joint With Combined Humeral Head and Glenoid Defects: A Cadaveric Study", The American Journal of Sports Medicine, vol. 44, no. 4, pp. 933–940, Apr. 2016.

[10] I. Polyzois, R. Dattani, R. Gupta, O. Levy, and A. A. Narvani, "Traumatic First Time Shoulder Dislocation: Surgery vs Non-Operative Treatment", The archives of bone and joint surgery, 4(2), 104–108, 2016.

[11] R. Abrams and H. Akbarnia, "Shoulder Dislocations Overview", In: StatPearls. Treasure Island (FL): StatPearls Publishing, 2020.

[12] D.Trofa, A. C. Hsu, W. N. Levine, "13 - Persistent anterior shoulder instability following surgical stabilization", Shoulder and Elbow Trauma and its Complications, R. M. Greiwe, Woodhead Publishing: 271-290, 2015.

[13] A.Hardy, V. Sabatier, P. Laboudie, B. Schoch, G. Nourissat, P. Valenti, J. Kany, J. Deranlot, N. Solignac, P. Hardy, M. Vigan and J. D. Werthel, "Outcomes After Latarjet Procedure: Patients with First-Time Versus Recurrent Dislocations", The American Journal of Sports Medicine, 48(1), pp. 21–26, 2020.

[14] J. Pogorzelski, E. M. Fritz, J. A. Godin, A. B. Imhoff and P. J. Millett, "Nonoperative treatment of five common shoulder injuries" Obere Extremität 13, pp. 89–97, 2018.

[15] T. S. Ellenbecker and K. E. Wilk, "Sport therapy for the shoulder, Evaluation, Rehabilitation, and Return to Sport", SPORT THERAPY SERIES, Vol. 7597, 2017.

[16] S. Nakagawa, R. Ozaki, Y. Take, R. Iuchi and T. Mae, "Relationship between glenoid defects and Hill-Sachs lesions in shoulders with traumatic anterior instability", The American journal of sports medicine, 43(11), pp. 2763–2773, 2015.

[17] Y. Ye, W. You, W. Zhu, J. Cui, K. Chen and D. Wang, "The Applications of Finite Element Analysis in Proximal Humeral Fractures", Computational and mathematical methods in medicine, vol. 2017, 2017.

[18] M. Zheng, Z. Zou, P. J. Bartolo, C. Peach and L. Ren, "Finite Element Models of the Human Shoulder Complex: A Review of Their Clinical Implications and Modelling Techniques", International journal for numerical methods in biomedical engineering, 33(2), 2017.

[19] "Computer Methods in Biomechanics and Biomedical Engineering. Imaging and Visualization", Abstract book from the 16th International Symposium CMBBE and 4th Conference on Imaging and Visualization, New York City, USA, August 14-16, 2019.

[20] J. S. Shaha, J. B. Cook, D. J. Song, D. J. Rowles, C. R. Bottoni, S. H. Shaha and J. M. Tokish, "Redefining "critical" bone loss in shoulder instability: Functional Outcomes Worsen With "Subcritical" Bone Loss", The American journal of sports medicine, 43(7), pp. 1719–1725, 2015.

[21] E. Itoi, S. B. Lee, L. J. Berglund, L. L. Berge and K. N. An, "The effect of a glenoid defect on anteroinferior stability of the shoulder after Bankart repair: a cadaveric study", The Journal of bone and joint surgery, American volume, 82(1), pp. 35-46, 2000.

[22] S. G. Kaar, S. D. Fening, M. H. Jones, R. W. Colbrunna and A. Miniaci, "Effect of humeral head defect size on glenohumeral stability: A cadaveric study of simulated Hill-Sachs defects", The American journal of sports medicine, 38(3), pp. 594-599, 2010.

[23] J. K. Sekiya, A. C. Wickwire, J. H. Stehle and R. E. Debski, "Hill-Sachs defects and repair using *osteoarticular ransplantation: biomechanical analysis using a joint compression model", The American journal of sports medicine, 37(12), pp.2459*-2466, 2009.

[24] P. Walia, A. Miniaci, M. H. Jones and S. D. Fening, "Influence of Combined Hill-Sachs and Bony Bankart Defects on Range of Motion in Anterior Instability of the Shoulder in a Finite Element Model*, Arthroscopy: The Journal of Arthroscopic & Related Surgery, 31(11), pp. 2119-2127, 2015.

[25] R. S. Snell, "Clinical anatomy by regions", 9th ed., Chapter 1, 2012.

[26] F. H. Martini, R. B. Tallitsch and J. L. Nath, "Human Anatomy", 9th ed, Pearson Education, 2018.

[27] "Anatomical Directional Terms". Available: https://ebsco.smartimagebase.com/search?q=anatomical+directional+terms&invert=1. Accessed on 18/September/2019.

[28] R. L. Drake, "Gray's Atlas of Anatomy", Philadelphia, PA :Churchill Livingstone, Chapter 7, 2015.

[29] A. B. Imhoff, J. B. Ticker and A. D. Mazzocca, "Atlas of Advanced Shoulder Arthroscopy", 3rd ed. Taylor & Francis Group, 2018.

[30] R. Drake, A. W. Vogl and A. Mitchell, "Gray's anatomy for students" Philadelphia: Elsevier/Churchill Livingstone, 2014.

[31] W. B. Kibler, "The role of the scapula in athletic shoulder function", The American journal of sports medicine, 26(2), pp. 325-337, 1998.

[32] S. J. Hall, "Basic biomechanics", New York, NY: McGraw-Hill, Chapter 7, 2007.

[33] P. Walia, A. Miniaci, M. H. Jones and S. D. Fening, "Theoretical model of the effect of combined glenohumeral bone defects on anterior shoulder instability: A finite element approach", Journal of Orthopaedic Research, 31(4), pp. 601-607, 2013.

[34] "Scapulothoracic joint" Available: https://www.kenhub.com/en/library/anatomy/scapulothoracic-joint. Accessed on 17/August/2020.

[35] R. Lugo, P. Kung and C. B. Ma, "Shoulder biomechanics", European journal of radiology, 68(1), pp. 16-24, 2008.

[36] S. M. Moore, P. J. McMahon, E. Azemi and R. E. Debski, "Bi-directional mechanical properties of the posterior region of the glenohumeral capsule", 38(6), pp. 1365-1369, 2005.

[37] D. R. Armfield, R. L. Stickle, D. D. Robertson, J. D. Towers and R. E. Debski, "Biomechanical Basis of Common Shoulder Problems", Seminars in musculoskeletal radiology, 7(1), pp. 5-18, 2003.

[38] M. Ramachandran, "Basic Orthopaedic Sciences", London: CRC Press, 2017.

[39] M. Marieswaran, I. Jain, B. Garg, V. Sharma and D. Kalyanasundaram, "A Review on Biomechanics of Anterior Cruciate Ligament and Materials for Reconstruction", Applied Bionics and Biomechanics, vol. 2018, 2018.

[40] A. Maciel, "Biomechanics of Hip Joint Capsule", 2002.

[41] Z. Yang, "Finite Element Analysis for Biomedical Engineering Applications", pp. 46-47, 2019.

[42] N. Bakshi and M. T. Freehill, "The Overhead Athletes Shoulder", Sports medicine and arthroscopy review, 26(3), pp. 88–94, 2018.

[43] D. F. Massimini, P. J. Boyer, R. Papannagari, T. J. Gill, J. P. Warner and G. Li, "In-vivo glenohumeral translation and ligament elongation during abduction and abduction with internal and external rotation", Journal of orthopaedic surgery and research, 7, 29, 2012.

[44] "Pathology and biomechanics of posterior instability" Available: https://musculoskeletalkey.com/pathology-and-biomechanics-of-posterior-instability/. Accessed on 05/June/2020.

[45] A. M. Halder, E. Itoi and K. N. An, "Anatomy and biomechanics of the shoulder", The Orthopedic clinics of North America, 31(2), pp. 159-176, 2000.

[46] D. P. Browe, C. A. Voycheck, P. J. McMahon and R. E. Debski, "Changes to the mechanical properties of the glenohumeral capsule during anterior dislocation", Journal of biomechanics, 47(2), pp. 464–469, 2014.

[47] D. C. Taylor and R. A. Arciero, "Pathologic changes associated with shoulder dislocations. Arthroscopic and physical examination findings in first time, traumatic anterior dislocations", The American journal of sports medicine, 25(3), pp. 306-311, 1997.

[48] M. J. Bollier and R. Arciero, "Management of glenoid and humeral bone loss", Sports Medicine and Arthroscopy Review. 18(3), pp.140-148, 2010.

[49] R. M. Degen, J. W. Giles, S. R. Thompson, R. B. Litchfield and G. S. Athwal, "Biomechanics of Complex Shoulder Instability", Clinics in sports medicine, 32(4), pp. 625-636, 2013.

[50] P. Boileau, M. Villalba, J. Y. Héry, F. Balg, P. Ahrens and L. Neyton, "Risk factors for recurrence of shoulder instability after arthroscopic Bankart repair", The Journal of bone and joint surgery, American volume, 88(8), pp. 1755–1763, 2006.

[51] "Bankart lesion and Hill-Sachs lesion". Available: http://pathologies.lexmedicus.com.au/pathologies/bankart-lesion-and-hill-sachs-lesion. Accessed on 15/November/2019.

[52] L. U. Bigliani, R. G. Pollock, L. J. Soslowsky, E. L. Flatow, R. J. Pawluk and V. C. Mow, "Tensile properties of the inferior glenohumeral ligament", Journal of orthopaedic research, 10(2), pp. 187-197, 1992.

[53] G. Di Giacomo, N. de Gasperis and P. Scarso, "Bipolar bone defect in the shoulder anterior dislocation", Knee surgery, sports traumatology, arthroscopy, 24(2), pp. 479–88, 2016.

[54] C. Simpfendorfer, M. Schickendantz and J. Polster, "The Shoulder: What is New and Evidence-Based in Orthopedic Sports Medicine", Current Radiology Reports, 2017.

[55] C. M. Robinson, J. Howes, H. Murdoch, E. Will and C. Graham, "Functional outcome and risk of recurrent instability after primary traumatic anterior shoulder dislocation in young patients" The Journal of bone and joint surgery, American volume, 88 (11), pp. 2326–2336, 2006.

[56] "Operative techniques in Orthopaedic Surgery". Available: ttps://doctorlib.info/surgery/operative-techniques-orthopaedic-surgery/364.html. Accessed on 30/November/2019.

[57] T.Y. Chuang, C. R. Adams and S. S. Burkhart, "Use of preoperative three-dimensional computed tomography to quantify glenoid bone loss in shoulder instability", Arthroscopy: the journal of arthroscopic & related surgery, 24 (4), pp. 376–382, 2008.

[58] A. Bhatnagar, S. Bhonsle and S. Mehta, "Correlation between MRI and arthroscopy in diagnosis of shoulder pathology", Journal of clinical and diagnostic research, 10(2), RC18-RC21, 2016.

[59] J. W. Galvin, J. J. Ernat, B. R. Waterman, M. J. Stadecker and S. A. Parada, "The Epidemiology and Natural History of Anterior Shoulder Instability", Current reviews in musculoskeletal medicine, 10(4), pp. 411–424, 2017.

[60] I. K. Lo, B. Nonweiler, M. Woolfrey, R. Litchfield and A. Kirkley, "An Evaluation of the Apprehension, Relocation, and Surprise Tests for Anterior Shoulder Instability" The American journal of sports medicine, 32(2), pp. 301-307, 2004.

[61] L. U. Bigliani, P. M. Newton, S. P. Steinmann, P. M. Connor and S. J. McIlveen, "Glenoid rim lesions associated with recurrent anterior dislocation of the shoulder", The American journal of sports medicine, 26(1), pp. 41-45, 1998.

[62] G. H. Garcia, H. H. Wu, J. N. Liu, G. R. Huffman and J. D. Kelly, "Outcomes of the remplissage procedure and its effects on return to sports: average 5-year follow-up", The American journal of sports medicine, 44(5), pp. 1124-1130, 2016.

[63] G. Milano, G. Frizziero and G. Marchi, "Bony Defects: Glenoid and Humeral Side—On-Track/Off-Track Concept", In: Brzóska, R., Milano, G., Randelli, P., Kovačič, L. (eds) 360° Around Shoulder Instability. Springer, Berlin, Heidelberg, 2020.

[64] X. Liu and L. Zhang, " Structural Theory. Bridge Engineering Handbook", Ed. Wai-Fah Chen and Lian Duan Boca Raton: CRC Press, Chapter 7, 2000.

[65] G.R. Liu and S.S. Quek, "The finite element method: a practical course", Butterworth-Heinemann, 2013.

[66] D. W. Pepper and J. C. Heinrich, "The Finite Element Method. Basic Concepts and Applications with MATLAB, MAPLE, and COMSOL", Taylor & Francis Group, Third Edition, 2017.

[67] S. K. Parashar and J. K. Sharma, "A review on application of finite element modelling in bone biomechanics", Perspectives in Science, 8, pp. 696-698, 2016.

[68] G. P. Nikishkov, "Introduction to the Finite Element Method", 2004.

[69] A. E. Tekkaya and C. Soyarslan, "Finite Element Method", In: The International Academy for Production Engineering, Laperrière L., Reinhart G. (eds) CIRP Encyclopedia of Production Engineering. Springer, Berlin, Heidelberg. 2014.

[70] A. N. Correia. "Estudo da Biomecânica do Ombro". MS, Faculdade de Engenharia, Universidade do Porto, 2011.

[71] R. E. Debski, S. M. Moore, J. L. Mercer, M. S. Sacks and P. J. McMahon, "The collagen fibers of the anteroinferior capsulolabrum have multiaxial orientation to resist shoulder dislocation." Journal of Shoulder and Elbow Surgery, 12(3), pp. 247-252. 2003.

[72] S. M. Moore, B. Ellis, J. A. Weiss, P. J. McMahon and R. E. Debski, "The glenohumeral capsule should be evaluated as a sheet of fibrous tissue: a validated finite element model", Annals of biomedical engineering, 38(1), pp. 66–76, 2010.

[73] C. Yongpravat, "Pre-Surgical Planning of Total Shoulder Arthroplasty and Glenohumeral Instability Repair Using Patient-Specific Computer Modeling", Ph.D., Columbia University, 2015.

[74] J. A. Weiss and J. C. Gardiner, "Computational Modeling of Ligament Mechanics," Critical reviews in biomedical engineering, 29(3), pp. 303-371, 2001.

[75] A.F. Bower, "Applied mechanics of solids", CRC press, 2009.

[76] M. Smith, "ABAQUS/Standard User's Manual", Version 6.9, Dassault Systèmes Simulia Corp, 2009.

[77] M. C. Fonseca. "Biomechanical Simulation of the Damage on the ACL in Injury Related Movements". MS, Faculdade de Engenharia, Universidade do Porto, 2020.

[78] B. Calvo, E. Peña, M. A. Martinez and M. Doblaré, "An uncoupled directional damage model for fibred biological soft tissues. Formulation and computational aspects", International Journal for Numerical Methods in Engineering, 69, pp. 2036 – 2057, 2007.

[79] J. P. S. Ferreira, M. P. L. Parente, M. Jabareen and R. N. Jorge, "A general framework for the numerical implementation of anisotropic hyperelastic material models including non-local damage", Biomechanics and modeling in mechanobiology, 16(4), p. 1119-1140, 2017.

[80] M. J. Bey, S. A. Hunter, N. Kilambi, D. L. Butler and T. N. Lindenfeld, "Structural and mechanical properties of the glenohumeral joint posterior capsule", Journal of Shoulder and Elbow Surgery, 14(2), pp. 201-206, 2005.